KDM5B histone demethylase controls epithelial-mesenchymal transition of cancer cells by regulating the expression of the microRNA-200 family.

Zanabazar Enkhbaatar[1,*], Minoru Terashima[1,*], Dulamsuren Oktyabri[1], Shoichiro Tange[1], Akihiko Ishimura[1], Seiji Yano[2], Takeshi Suzuki[1,†]

[1]Division of Functional Genomics, [2]Division of Medical Oncology, Cancer Research Institute, Kanazawa University, Kanazawa 920-1192, Ishikawa, Japan

[*] These authors contributed equally to this study

[†] To whom correspondence should be addressed

Takeshi Suzuki, Division of Functional Genomics, Cancer Research Institute, Kanazawa University, Kakuma-machi, Kanazawa 920-1192, Ishikawa, Japan

Phone: +81-76-264-6741; Fax: +81-76-234-4502; E-mail: suzuki-t@staff.kanazawa-u.ac.jp

Disclosure Statement

The authors have no conflict of interest.

Key words

Tumor progression; Histone methylation; Transcription; microRNA;

Epithelial-mesenchymal transition

Abbreviations

DMEM, Dulbecco's modified Eagle's medium; FBS, fetal bovine serum; GAPDH, glyceraldehyde-3-phosphate dehydrogenase; H3K4me3, histone H3 tri-methylated Lys4; HEK293T cells, human embryonic kidney cells expressing the large T-antigen of simian virus 40; IgG, immunoglobulin G; miRNA, microRNA; shRNA, small hairpin RNA; EMT, epithelial-mesenchymal transition; TGF-β, Transforming Growth Factor-beta; ChIP, chromatin immunoprecipitation

Running title

Role of KDM5B histone lysine demethylase in EMT

Abstract

Histone methylation is implicated in various biological and pathological processes including cancer development. In this study, we discovered that ectopic expression of KDM5B, a histone H3 lysine 4 (H3K4) demethylase, promoted epithelial-mesenchymal transition (EMT) of cancer cells. KDM5B increased the expression of transcription factors, ZEB1 and ZEB2, followed by down-regulation of E-cadherin and up-regulation of mesenchymal marker genes. The expression of the microRNA-200 (miR-200) family, which specifically targets ZEB1 and ZEB2, was reduced in the cells with KDM5B overexpression. We found that KDM5B repressed the expression of the miR-200 family by changing histone H3 methylation status of their regulatory regions. The introduction of miR-200 precursor in the cells inhibited EMT induction by KDM5B, suggesting that miR-200 family was a critical downstream mediator of KDM5B-promoted EMT. Furthermore, knockdown of KDM5B was shown to affect the expression of EMT-related genes, indicating the involvement of endogenous KDM5B. Our study demonstrated a novel role of KDM5B histone lysine demethylase in EMT, which may contribute to malignant progression of cancer.

Introduction

Histone modifications such as acetylation, phosphorylation and methylation can function individually or in combination to elicit specific effects on chromatin structure and gene expression.[1] Histone lysine (K) methylation, in particular, has emerged as an important modification due to its central role in transcriptional regulation. [2, 3] Histone lysine methylation is associated with activated or repressed transcription of individual genes depending on the methylated residue and the degree of methylation, since lysine residues can be mono-, di- or tri-methylated (me1, me2 or me3). [4, 5] Moreover, a given methylated mark is often linked to a specific position of the gene, either around the transcription initiation site or in the coding region, regulating transcriptional initiation or elongation. In general, methylation of lysine-4 of histone H3 (H3K4) around TSS and methylation of H3K36 and H3K79 on the coding region are associated with active transcription. Methylation of H3K9 and H3K27 on promoters correlates with transcriptional repression.[6, 7] The discovery of a large number of site-specific histone methyltransferases and demethylases reveals the dynamic regulation of histone methylation.[4, 5] Reversible histone lysine methylation is implicated in diverse biological processes including cellular

proliferation, differentiation, DNA repair and recombination. The importance of the tight regulation of histone methylation is demonstrated by emerging links of histone methylation to human disease such as cancer.[4]

Identification of genes involved in cancer gives us crucial information about the molecular mechanism of cancer development. Genetic screens for mutations contributing to tumor formation in model organisms facilitate the efficient identification of cancer genes in an *in vivo* setting. Retroviral insertional mutagenesis in mice is one of the potent cancer gene discovery tools. [8] Previously we have accomplished high-throughput cloning of retroviral integration sites from the tumors of murine leukemia virus (MuLV)-infected mice. This screen led to the identification of hundreds of candidate cancer genes including many genes encoding histone lysine methyltransferases and demethylases.[9, 10] These results provided us with an opportunity to explore the functions of these enzymes in the course of cancer development. Previously, we reported that JMJD2C, a histone H3K9 demethylase, increased the expression of *MDM2* oncogene, resulting in the reduction of p53 tumor suppressor in the cells.[11] We also showed that UTX H3K27 demethylase enhanced the expression of *RB1* and *RBL2* genes that play important roles in cell proliferation.[12] In

addition, we demonstrated that KDM5B/PLU1 H3K4 demethylase repressed the expression of *KAT5/TIP60* and *CD82/KAI1* genes, thereby increasing the invasive activity of the cancer cells.[13] Thus our studies revealed that histone methyl-modifying enzymes were involved not only in tumor initiation but also in tumor progression such as invasion and metastasis.

The increased motility and invasiveness of malignant tumor cells are often associated with epithelial-mesenchymal transition (EMT) of the cells.[14, 15] Loss of E-cadherin-mediated cell interaction is the most important step and a well-known marker for EMT. The up-regulation of mesenchymal markers such as Fibronectin and N-cadherin also characterizes EMT process. Many studies on the molecular mechanisms for E-cadherin repression have revealed that several transcription factors including SNAI1, SNAI2, ZEB1, ZEB2 and TWIST, are involved in the complex network that regulate EMT.[16–18] EMT is a dynamic and reversible process that primarily occurs at the invasive front of the tumor. When cancer cells distribute to distant sites of the body, they can revert to an epithelial state via mesenchymal-epithelial transition. The plasticity of EMT suggests that epigenetic regulation such as DNA methylation and histone modification is implicated in the EMT

process.[19, 20] Recent reports indicated the connection between EMT and histone methylation. SNAI1 was shown to interact with LSD1 H3K4 demethylase or G9A H3K9 methyltransferase and recruited them to *CDH1/E-cadherin* promoter for transcriptional repression during EMT.[21, 22] However, the exploration for the role of histone methyltransferase or demethylase in EMT has just begun.

Histone H3K4 demethylase KDM5B/PLU1/JARID1B has been reported to play important roles in cancer development, since up-regulation of KDM5B was observed in many types of malignant tumors.[23–26] Previously we reported that KDM5B enhanced the invasive potential of cancer cells, clarifying its function in malignant tumor progression.[13] However, the involvement of KDM5B in other processes of cancer progression such as EMT remained unknown.

In this paper we demonstrated that overexpression of KDM5B promoted the EMT process of cancer cells. KDM5B specifically increased the expression of ZEB1 and ZEB2 transcription factors, the critical regulators of EMT induction. Mechanistic investigations indicated that KDM5B regulated the expression of microRNA-200 family targeting ZEB1 and ZEB2 transcripts through the changes of histone H3 methylation on their regulatory

regions.

Results

Ectopic expression of KDM5B induced morphological changes of the cells

Previously, we demonstrated that KDM5B/PLU1 histone lysine demethylase played an important role in the cell invasion process of cancer progression.[13] To investigate the involvement of KDM5B in other processes of malignant progression, we examined whether ectopic expression of KDM5B would affect epithelial-mesenchymal transition (EMT) of cancer cells. We used a lung cancer cell line, A549, because it shows clear morphological changes during EMT caused by the treatment of Transforming Growth Factor-beta (TGF-β).[29] A549 cells were infected with the retroviruses expressing either without insert or with FLAG-tagged wild-type KDM5B or catalytically inactive KDM5B mutant H499Y, [13, 25] and the infected cells were selected in the medium containing 800μg/ml of G418. The cell lysates of the infected cells were prepared and subjected to Western blot analysis with anti-FLAG antibody (Fig. S1A). We confirmed that exogenously introduced wild-type and mutant KDM5B proteins were produced at a similar level in A549 cells (Fig. S1A).

As a positive control for EMT induction, we used A549 cells treated with TGF-β for 48 hours. After TGF-β treatment, the cells were dispersed, elongated and assumed a

fibroblast-like appearance (Fig. 1A, Control plus TGF-β). Similar morphological changes of A549 cells were observed with the expression of wild-type KDM5B but not of inactive KDM5B mutant (Fig. 1A, KDM5B WT and Mut), suggesting that overexpression of KDM5B might induce EMT. To confirm this, we performed immunofluorescence assay for A549 cells using an antibody against E-cadherin, an epithelial cell marker. Untreated A549 cells showed heterogeneous E-cadherin staining (Fig. 1B, Control), and this staining was almost lost in TGF-β-treated cells (Fig. 1B, Control plus TGF-β) as described in the previous reports.[29] We discovered that E-cadherin staining significantly reduced in the cells with the expression of wild-type KDM5B (Fig. 1B, KDM5B WT). No significant change was observed after infection with the virus expressing the inactive mutant (Fig. 1B, KDM5B Mut). These results indicated that the epithelial property of the cells might be lost by the expression of wild-type KDM5B. We further examined the status of actin in the cells by TRITC-conjugated phalloidin staining, since actin reorganization occurs during the EMT process.[17] In contrast to untreated cells (Fig. 1C, Control), treatment of TGF-β dramatically induced actin fiber formation typical of EMT (Fig. 1C, Control plus TGF-β). Phalloidin staining revealed a similar actin fiber formation in the cells with wild-type

KDM5B, but not with the inactive mutant (Fig. 1C, KDM5B WT and Mut).

We next examined whether KDM5B overexpression would cause similar effects on other EMT models. We used a mouse mammary epithelial cell line, NMuMG, and a human colon cancer cell line, HT29, because these cell lines respond to TGF-β for EMT induction. We first confirmed the expression level of wild-type and mutant KDM5B proteins in NMuMG cells (Fig. S1B) and HT29 cells (Fig. S1C). The expression of wild-type KDM5B but not its mutant induced similar morphological changes of NMuMG cells (Fig. S2A) and HT29 cells (Fig. S3A) as TGF-β treatment did. Moreover, the cells with wild-type KDM5B showed disappearance of E-cadherin staining and formation of actin stress fiber (Fig. S2B, S2C, S3B and S3C). Altogether, these results indicated that ectopic expression of KDM5B caused morphological changes and cytoskeletal rearrangement consistent with EMT in A549 lung cancer cells, NMuMG mammary epithelial cells and HT29 colon cancer cells, which was dependent on its demethylase activity.

KDM5B affected the expression of EMT related genes

Besides the reduction of E-cadherin, EMT is characterized by up-regulation of

mesenchymal marker genes.[14, 15, 17] Therefore we analyzed the expression of two representative mesenchymal marker genes, *FN1/Fibronectin* and *CDH2/N-cadherin*, as well as an epithelial marker, *CDH1/E-cadherin*, in the cells with KDM5B expression. Quantitative RT-PCR analysis revealed that TGF-β treatment decreased the expression of *CDH1* mRNA in A549 cells (Fig. 2A) as previously reported.[29] Expression of wild-type KDM5B similarly reduced the *CDH1* expression, but its mutant had no effect (Fig. 2A). On the other hand, for *FN1* or *CDH2* whose expression was elevated by TGF-β, wild-type KDM5B increased their expression significantly, but the mutant did not change the expression (Fig. 2B and 2C). These results again indicated that the effect was dependent on the demethylase activity of KDM5B. Judging from the changes in the epithelial and mesenchymal marker gene expression, we could conclude that overexpression of wild-type KDM5B induced EMT of A549 cells.

During the EMT process, it has been reported that the expression of E-cadherin is regulated by multiple transcriptional repressors.[16, 17] Thus we investigated whether overexpression of KDM5B affected the expression of transcription factors such as SNAI1, SNAI2, ZEB1 and ZEB2. Quantitative RT-PCR analysis showed that TGF-β treatment

up-regulated the expression of all transcription factors we examined in A549 cells (Fig. 2D, 2E, 2F and 2G). Expression of wild-type KDM5B did not affect the expression of *SNAI1* and *SNAI2* significantly (Fig. 2D and 2E), but resulted in the increased expression of *ZEB1* and *ZEB2* in A549 cells (Fig. 2F and 2G). We also confirmed the changes of protein expression for some of the EMT-related gene products in A549 cells. Western blot showed that the expression of wild-type KDM5B resulted in the reduction of E-cadherin protein and the increase of ZEB1 and ZEB2 proteins as TGF-β treatment did (Fig. 2H).

Quantitative PCR and Western blot revealed that KDM5B overexpression induced essentially the same changes for the EMT-related gene expression in NMuMG mammary epithelial cells (Fig. S4A to S4H), although endogenous ZEB2 protein was not detected because of its extremely low expression in NMuMG cells. Moreover, in HT29 colon cancer cells, KDM5B resulted in the similar changes for the EMT-related gene expression (Fig. S5A to S5E), although endogenous expression of *CDH2/N-cadherin, SNAI2* and *ZEB2* was extremely low or not detected in HT29 cells. These results together suggested that KDM5B histone lysine demethylase might be specifically involved in the regulation of ZEB family expression and then control the transcriptional network leading to EMT.

KDM5B did not seem to be directly involved in the expression of *CDH1/E-cadherin*, *ZEB1* or *ZEB2*

Since KDM5B is an enzyme that possesses a demethylase activity of histone H3 to regulate gene expression,[23–25] we examined the recruitment of KDM5B and the methylation status of histone H3 on the regulatory regions of *CDH1/E-cadherin*, *ZEB1* or *ZEB2* gene. Chromatin immunoprecipitation (ChIP) assay was performed using antibodies that specifically recognize methylated K residues of histone H3[28] or FLAG epitopes. A549 cells were infected with the control retrovirus or the retrovirus expressing FLAG-tagged wild-type KDM5B, and the cell lysates were prepared. Following immunoprecipitation, total ten different primer sets positioned upstream or around the transcription initiation sites of *CDH1*, *ZEB1* and *ZEB2* gene were used in quantitative PCR analysis (Fig. 3A, 3C, 3E, S6A, S7A and S8A). We analyzed the transcriptionally active tri-methylated H3K4 (H3K4me3) status and the repressive H3K27me3 status on the regulatory region of each gene. As a representative result for each gene locus, the data from one primer set (region a) was presented (Fig. 3B, 3D and 3F). The data obtained from all other primer sets were

shown in Fig. S6B, S7B and S8B. In the case of *CDH1* gene, H3K4me3 was significantly decreased and H3K27me3 was slightly increased in the regions around the transcription initiation site with the expression of wild-type KDM5B (Fig. 3B and S6B). Since *CDH1* expression was down-regulated by KDM5B, this observation was consistent with the previous report showing low level of H3K4me3 and high level of H3K27me3 on the regulatory regions were linked to transcriptionally repressed status.[6] However, the recruitment of KDM5B was not detected on the all regions of *CDH1* gene that we have tested (Fig. 3B and S6B). These results suggested that KDM5B did not seem to be directly involved in the transcriptional regulation of *CDH1*. On the other hand, we did not detect any significant changes of H3K4me3, H3K27me3 and the recruitment of KDM5B on the all regions of *ZEB1* and *ZEB2* genes that we have examined (Fig. 3D, 3F, S7B and S8B). These results might also exclude the direct involvement of KDM5B in the transcriptional regulation of *ZEB1* and *ZEB2* genes in the cells with KDM5B overexpression.

KDM5B regulated the expression of the microRNA-200 family gene through the conversion of histone H3 methylation

The finding that KDM5B increased *ZEB1* and *ZEB2* expression specifically and indirectly in the EMT process led us to investigate the possibility that the effect could be due to the regulation of the miR-200 family of microRNAs. The miR-200 family has been established as a key regulator of epithelial phenotype, and is known to be deeply involved in the EMT process.[30, 31] The miR-200 family was found to directly target and inhibit ZEB1 and ZEB2 specifically. Genetically, the miR-200 family is grouped in two polycistronic units: *miR-200b/200a/429* and *miR-200c/141*, clustered in chromosome 1 and 12, respectively (see Fig. 4C and 4E). Therefore we examined whether KDM5B overexpression would affect the expression of two representative microRNAs, miR-200a and miR-200c. Consistent with the previous reports,[30] quantitative RT-PCR revealed that TGF-β treatment resulted in a decreased expression of miR-200a and miR-200c in A549 cells (Fig. 4A and 4B). We could also detect a decrease in the expression of miR-200a and miR-200c with the expression of wild-type KDM5B but not with its mutant (Fig. 4A and 4B). The expression of miR-302a that belongs to an unrelated miR-302 family was not significantly affected by KDM5B expression (data not shown), suggesting the specific effect of KDM5B on the miR-200 family. We also found the similar down-regulation of

miR-200a and miR-200c induced by wild-type KDM5B in NMuMG cells and HT29 cells (Fig. S9). These results strongly suggested that KDM5B was implicated in the regulation of the miR-200 family expression and involved in the EMT process through this regulation.

Next we examined the methylation status of histone H3 on the regulatory regions of the miR-200 family genes by ChIP analysis. As shown in Fig. 4C and 4E, the transcription initiation sites of *miR-200b/200a/429* and *miR-200c/141* precursor RNAs were reported previously.[32, 33] Following immunoprecipitation, the two primer sets positioned around the transcription initiation sites of the microRNA clusters were used in quantitative PCR analysis (Fig. 4C and 4E). On the regulatory regions of both *miR-200b/200a/429* and *miR-200c/141* genes, the level of H3K4me3 was dramatically decreased by the expression of KDM5B (Fig. 4D and 4F). Moreover, ChIP assay using anti-FLAG antibody clearly demonstrated the increased occupancies of FLAG-tagged wild-type KDM5B on the regulatory regions (Fig. 4D and 4F). The level of repressive H3K27me3 mark was significantly increased by KDM5B expression (Figure 4D and 4F), which was correlated with the transcriptional repression by KDM5B. These results suggested that KDM5B which was recruited on the regulatory regions of *miR-200b/200a/429* and *miR-200c/141* genes

converted the chromatin structure to a more transcriptionally repressed status by demethylating H3K4. As a control experiment, we performed ChIP assay on the regulatory regions of *BRCA1* and *HOXA5* genes that were reported to be the target genes regulated by KDM5B[25] and also unrelated *GAPDH* gene (Fig. S10). In the case of *BRCA1* and *HOXA5* genes, the decrease of H3K4me3 and the increase of H3K27me3 were detected simultaneously with the recruitment of KDM5B on the regulatory regions (Fig. S10B and S10D). On the other hand, there were no significant changes in H3K4 and H3K27 methylation and KDM5B occupancies on the regulatory regions of *GAPDH* gene by KDM5B (Fig. S10F). These results indicated that KDM5B-induced changes of histone H3 methylation were specific to the target genes regulated by KDM5B including *miR-200b/200a/429* and *miR-200c/141* genes, which was closely correlated with the specificity of transcriptional regulation by KDM5B.

The regulation of miR-200 family expression was important in KDM5B-induced EMT

In order to clarify the role of the miR-200 family down-regulated by KDM5B in EMT, we transfected the precursor of miR-200a or miR-200c into KDM5B-expressing A549 cells

to see the rescue effects in the EMT process. Fig. 5A showed that the expression of wild-type KDM5B decreased *CDH1/E-cadherin* expression but simultaneous introduction of miR-200a or miR-200c precursor recovered *CDH1* expression. Transfection of miR-200a or miR-200c was also shown to inhibit the enhanced expression of mesenchymal marker *CDH2/N-cadherin* by KDM5B (Fig. 5B). These results suggested that over-expression of miR-200a or miR-200c inhibited EMT induction by KDM5B expression. Moreover, the expression of miR-200a or miR-200c counteracted the enhanced expression of *ZEB1* and *ZEB2* induced by KDM5B (Fig. 5C and 5D), but had no effect on the expression of *SNAI1* and *SNAI2* (data not shown). We found that the introduction of miR-200a or miR-200c precursor resulted in the loss of mesenchymal cell appearance of the KDM5B-expressing cells by the staining of E-cadherin and actin (Fig. S11A and S11B). We also confirmed that the expression of miR-200a or miR-200c did not affect the expression level of KDM5B proteins (Fig. S12). These results clearly indicated the inhibitory function of these microRNAs in EMT process induced by KDM5B. Taken together, we could conclude that the reduced expression of miR-200a and miR-200c was primarily responsible for the EMT induction by KDM5B overexpression.

Knockdown of KDM5B indicated the involvement of endogenous KDM5B in the transcriptional regulation of EMT-related genes

To extend our understanding for the regulation of EMT by KDM5B, we examined the effects of KDM5B knockdown in the cells. We used the retroviruses expressing small hairpin RNA (shRNA) for efficient and stable knockdown of KDM5B as described previously.[13] A549 cells were infected with the control retrovirus or the retrovirus expressing KDM5B shRNA, and we examined the expression of *CDH1/E-cadherin*, *FN1/Fibronectin* and *CDH2/N-cadherin* in the cells with KDM5B knockdown by quantitative RT-PCR. Knockdown of KDM5B increased the *CDH1* expression, but decreased the expression of *FN1* and *CDH2* (Fig. 6A, 6B and 6C). These results indicated that KDM5B knockdown resulted in the opposite effects compared to KDM5B overexpression. By immunofluorescence, KDM5B knockdown induced stronger staining of E-cadherin on the cell membrane compared to control cells (Fig. S13A, KDM5B sh *versus* Control), but had no effect on actin organization (Fig. S13B). Next we examined the expression of EMT-related transcription factors by quantitative RT-PCR and found that

KDM5B knockdown decreased the expression of *ZEB1* and *ZEB2* (Fig. 6D and 6E). We also confirmed the corresponding changes of protein expression for E-cadherin, ZEB1 and ZEB2 in A549 cells by KDM5B knockdown (Fig. 6F). Furthermore, we found that the expression of miR-200a and miR-200c was elevated in the KDM5B knockdown cells (Fig. 6G and 6H). From the ChIP experiments, we could detect the increase of H3K4me3 and the decrease of H3K27me3 on the regulatory regions of *miR-200b/200a/429* and *miR-200c/141* genes induced by KDM5B knockdown (Fig. 6I and 6J). These results indicated that endogenous KDM5B was involved in the transcriptional regulation of EMT-related genes in A549 cells. Next we examined whether KDM5B knockdown could be refractory to TGF-β-induced EMT process. KDM5B knockdown did not affect the loss of E-cadherin staining and actin fiber formation induced by TGF-β (Fig. S13A and S13B, KDM5B sh plus TGF-β *versus* Control plus TGF-β). Based on the quantitative PCR analyses for EMT-related gene expression, KDM5B knockdown did not counteract with TGF-β-induced changes of gene expression, either (Fig. S14A to S14E). Finally, it was shown that the level of endogenous KDM5B was slightly but significantly increased after TGF-β treatment in A549 cells (Fig. S15). Taken together, these results suggested that endogenous KDM5B

played an important role in the transcriptional regulation of EMT-related genes possibly through the regulation of the miR-200 family expression, although TGF-β treatment could overcome the depletion of KDM5B for the induction of EMT of the cells.

Significant association between *KDM5B* and *ZEB* family expression in human lung cancer tissues

The finding that KDM5B resulted in the increased expression of ZEB family transcription factors led us to examine the correlation between *KDM5B* and *ZEB* family expression in human cancer specimens. Quantitative RT-PCR analysis was performed to detect the expression of *KDM5B, ZEB1* and *ZEB2* in human lung cancer tissues (N=24). To determine the possible relationship of *KDM5B* and *ZEB* family, we compared the gene expression results using Pearson correlation coefficient. As shown in Fig. 7, each dot represented the values of two genes (i.e., x-and y-axis) and the correlation coefficient reflected an association between the two genes. We detected a significant association of *KDM5B* and *ZEB1* expression (Fig. 7A) or *KDM5B* and *ZEB2* expression (Fig. 7B). The associations were positive with r=0.442 ($P < 0.05$) and with r=0.601 ($P < 0.005$),

respectively. These results suggested that KDM5B might regulate the expression of *ZEB* family, one of the critical EMT inducers, during the development of human lung cancer.

DISCUSSION

In the current study, we found that ectopic expression of KDM5B H3K4 demethylase enhanced the expression of *ZEB1* and *ZEB2* and resulted in decreased *CDH1/E-cadherin* expression, thereby promoting EMT. This effect of KDM5B was commonly observed in several EMT model systems including A549 human lung cancer cells, HT29 colon cancer cells and NMuMG mouse mammary epithelial cells. KDM5B was shown to regulate the expression of the microRNA-200 family, which specifically inhibits ZEB1 and ZEB2, through the conversion of histone H3 methylation on their regulatory regions. We also showed that knockdown of KDM5B affected the expression levels of EMT-related genes, suggesting the involvement of endogenous KDM5B. Moreover, we detected a positive association between *KDM5B* and *ZEB* family expression in human lung cancer tissues. Our study uncovers a novel role of KDM5B histone lysine demethylase in EMT, and has important implication in targeting cancer metastasis.

A growing body of evidence indicates that overexpression or mutations of histone methyltransferases and demethylases have been linked to the development of many human cancers.[4] A histone H3K27 methytransferase, EZH2, and H3K4 demethylases, LSD1 and

KDM5B have been thought to play important roles not only in tumor initiation but also in tumor progression, since overexpression of these genes has been reported in many types of malignant tumors. [24, 26, 34–37] Previous papers revealed that up-regulation of EZH2 or LSD1 enhanced cell migration, cell invasion and EMT to promote malignant progression of cancer cells.[35, 36] During the EMT process, it was shown that EZH2 repressed E-cadherin gene expression[35] and that LSD1 interacted with SNAI1 to repress E-cadherin and other epithelial genes.[21] Although we previously reported that overexpression of KDM5B/PLU1 enhanced the invasive potential of cancer cells through repressing *KAT5* and *CD82* expression,[13] the involvement of KDM5B in EMT remained unknown. Here we identified a novel important role of KDM5B that contributed to EMT, another hallmark of cancer aggressiveness. Overexpression of KDM5B was shown to promote the EMT process of the cells by increasing the expression of ZEB1 and ZEB2 transcription factors through the regulation of microRNA-200 family expression. Moreover, we have observed KDM5B-induced EMT both in cancer cells, A549 and HT29, and benign epithelial cells, NMuMG, which might ensure the generality of novel function of KDM5B.

The members of the miR-200 family are important regulators of EMT. Deregulation of

miR-200 family expression occurred in multiple types of cancer cells and was linked to tumor progression.[30, 31] It was proposed that the expression of miR-200 family was controlled by epigenetic mechanisms.[33, 38] Increased EZH2 activity in cancer was shown to cause repression of numerous microRNAs including miR-200b and miR-200c through H3K27me3 regulation at these loci.[39] A recent paper also demonstrated that knockdown of JMJD3 H3K27 demethylase decreased the expression of miR-200b and miR-200c for up-regulation of EMT inducers such as ZEB1 and ZEB2,[40] suggesting the importance of H3K27 methylation in the regulation of miR-200 family expression. Furthermore, a recent genome-wide profiling of histone methylation during EMT revealed strong correlations between the dynamic changes of histone methylations and gene expression.[19] For genes with bivalent marks with H3K4me3 and H3K27me3, the level of transcription was shown to be dependent on the relative intensities of active H3K4me3 and repressive H3K27me3 marks. This was closely correlated with our results of ChIP experiments: overexpression of KDM5B induced the decrease of H3K4me3 and the increase of H3K27me3 on the regulatory regions of the miR-200 family, resulting in decreased expression, but KDM5B knockdown caused the opposite changes of histone methylations for the increased

expression of the miR-200 family.

KDM5B has been found highly expressed in various types of tumors such as breast, prostate, bladder and lung cancers. [23, 24, 26] Increased expression of KDM5B caused proliferation in breast cancer and depletion of KDM5B inhibited tumor growth in a mouse mammary tumor model.[25] KDM5B can demethylate H3K4me3/me2 and was shown to regulate the expression of various cellular genes including BRCA1 tumor suppressor, E2F1 and E2F2 genes.[25, 26] In this study, we identified miR-200 family genes as the novel target genes regulated by KDM5B. Overexpression of KDM5B led to the repression of miR-200 family genes and KDM5B knockdown increased their expression. The recruitment of KDM5B and the changes of histone H3 methylation could be detected on the regulatory regions of miR-200 family genes like the cases of *BRCA1* and *HOXA5* genes that have been already reported as KDM5B-targets. Furthermore, introduction of miR-200 precursor was shown to inhibit EMT phenotype of the cells induced by KDM5B. These findings strongly suggested that miR-200 family was an important downstream mediator of KDM5B-induced EMT, although we could not rule out the possibility that other target genes regulated by KDM5B might be also involved in EMT.

We have also detected that ectopic expression of KDM5B increased the cell invasion activity of A549 lung cancer cells and repressed the expression of other KDM5B target genes, *KAT5* and *CD82*, that we previously described ([13] and unpublished results). Since CD82 is involved in integrin-mediated cell migration, these results suggested that KDM5B might affect both EMT and integrin-mediated pathway leading to cell invasion in A549 cells. However, in MCF10A immortalized breast epithelial cells, KDM5B overexpression enhanced cell invasion, but had no effect in *CDH1* expression,[13] suggesting that EMT might not be necessary for cell invasion activity of MCF10A cells. Therefore, epigenetic regulation by KDM5B might be differently involved in EMT or cell invasion process in different type of cell lines. Further studies using various cancer cell lines would be required to extend our understanding for KDM5B function in malignant progression.

By the knockdown experiments for KDM5B, we provided the evidence supporting the role of endogenous KDM5B in the transcriptional regulation of EMT-related genes. KDM5B knockdown increased *CDH1* expression and decreased the expression of *ZEB1* and *ZEB2* through up-regulation of the microRNA-200 family. Alteration of histone H3 methylation on the regulatory regions of the microRNA clusters was suggested to be the

underlying mechanism, although the recruitment of endogenous KDM5B on the regulatory regions was not be detected probably due to the low level of protein expression or low sensitivity of the available antibodies. We found that endogenous KDM5B was slightly but significantly induced by TGF-β treatment in A549 cells, but KDM5B knockdown could not counteract with TGF-β-induced EMT process. However, this result did not weaken the importance of endogenous KDM5B function in EMT process. Since TGF-β operated at the upstream of signaling pathway and activated various signaling molecules, transcription factors and epigenetic regulators in the cells for EMT induction, it was possible that KDM5B knockdown could not interrupt the profound effects caused by TGF-β. Further studies would be essential to delineate the precise role of endogenous KDM5B in the process of EMT.

In this paper, we have shown the important function of KDM5B histone demethylase in EMT. The regulation of the miR-200 family expression through histone H3 methylation was shown to be a novel mechanism for KDM5B action. These findings strongly suggest that deregulation of histone methyl-modifying enzymes and microRNA expression contributes to a critical step for malignant progression of cancer. Our study reveals a novel

epigenetic mechanism regulating EMT and has important implications in devising novel targets for therapeutic interventions in the treatment of aggressive cancers.

Material and Methods

Plasmids, cell culture and transfection

The construction of the retrovirus vectors expressing mouse KDM5B or its inactive mutant H499Y was described previously.[13] To produce pantropic retroviruses for the infection of human cells, the retrovirus vectors were co-transfected into GP2-293 packaging cells (Takara) with pVSV-G plasmid (Takara) using FuGENE HD reagent (Roche). To produce ecotropic retroviruses for the infection of mouse cells, the retrovirus vectors were transfected into Plat-E packaging cells.[11] Forty-eight hours after transfection, the supernatants were collected. The retroviral stock was added into the medium with 6μg/ml polybrene (Sigma) for infection. The infected cells were selected in the medium containing 800μg/ml G418 (nacalai) for two to five days, and used for the experiments.

A549 human lung cancer cell line, HT29 human colon cancer cell line and NMuMG mouse mammary epithelial cell line were maintained in Dulbecco's modified Eagle's medium (DMEM) with 10% FBS, 2mM glutamine and penicillin/streptomycin (Sigma) at 37 ^{o}C in 5% CO2. For EMT induction, the cells were treated with 1 to 5 ng/ml of Transforming Growth Factor-beta (TGF-β) (R&D Systems) for 24 to 48 hours.

The construction of shRNA-expressing retrovirus vectors expressing KDM5B shRNA#1, #2 and control shRNA was described previously.[13] To produce shRNA-expressing retroviruses, the retrovirus vectors were co-transfected into HEK293T cells with MISSION Lentiviral Packaging Mix (Sigma-Aldrich). The infected cells were selected in the medium containing 500 ng/ml puromycin (Nacalai). As described previously,[13] the knockdown efficiencies of KDM5B shRNA #1 and #2 were 82% and 77% reduction compared to the control, respectively. We used these two effective shRNA-expressing retroviruses in this study and essentially obtained the same effects of both. Therefore we presented the data of KDM5B shRNA#1 as a representative result.

Transfections of miRNA precursors (Ambion) were carried out with Lipofectamine RNAiMAX (Invitrogen) by reverse transfection procedure. Cells were transfected with pre-miR-200a (#PM10991), pre-miR-200c (#PM11714) or negative control #1 (#AM17110) miRNA at a final concentration of 10 nM, and further incubated for three days and used for the experiments.

Patient samples

For gene expression studies, 24 tumor specimens were obtained from lung adenocarcinoma patients with written informed consent at Kanazawa University Hospital in Japan. RNA was obtained from the OCT-Compound-embedded frozen tissues (Tissue-Tek). The association between mRNA expressions was analyzed by Pearson correlation coefficient, and the results were summarized by scatter plot. All tests were two-sided and p-values < 0.05 were considered statistically significant. The experiment was approved by the Ethics Committee of Kanazawa University School of Medicine.

Quantitative PCR

RNA preparation and quantitative RT-PCR analysis were performed as described previously.[11] PCR data were normalized with respect to control human *GAPDH*, human *DDX5* or mouse *Actb* expression. The averages from at least three independent experiments are shown with the standard deviations. In the quantitative PCR experiments, Student's t-tests were used to determine the statistical significance of differences between samples treated under different conditions. Differences were considered statistically significant when $p < 0.05$. Primers used for the quantitative PCR were described previously

[13] and listed in Supplementary Table S1.

For microRNA quantification, TaqMan MicroRNA Assays (Applied Biosystems) for miR-200a (#000502), miR-200c (#002300) and miR-302a (#000529) were used according to the manufacture's protocol. The relative miRNA levels were calculated using the formula $2^{-\Delta\Delta Ct}$. All data were normalized with respect to the expression of *RNU6B* (#001093) for human or *snoRNA202* (#001232) for mouse.

Immunoblotting.

Cells were lysed in RIPA buffer as described previously.[27] The lysates were separated on SuperSep Ace 10% running gel (Wako) and transferred to Hybond™-LFP membrane (GE Healthcare). Anti-E-cadherin (#610181, BD Transduction Lab), anti-ZEB1 (#3396, Cell Signaling), anti-ZEB2 (#61096, Active Motif) and anti-GAPDH (6C5, Millipore) antibodies were used.

Chromatin immunoprecipitation (ChIP) assays

ChIP experiments were performed as previously described.[13, 28] The cross-linked

chromatins were immunopreciptated with mouse antibody (anti-H3K27me3, anti-H3K4me3, anti-FLAG (M2, Sigma) and normal IgG), and the complexes were collected by Dynabeads M-280 sheep anti-mouse IgG (Invitrogen). The enrichment of the specific amplified region was analyzed by quantitative PCR and percentage enrichment of each histone modification over input chromatin DNA was shown. The averages from at least three experiments are presented with the standard deviations.

Cell staining and immuno-fluorescence assay

To detect the morphological changes of the cells, A549 or NMuMG cells were fixed with 4% paraformaldehyde in phosphate-buffered saline (PBS) and stained with 0.4 % crystal violet (Waldeck). To allow direct fluorescence of actin cytoskeleton, A549 cells were fixed, permeabilized with 0.2% Triton X-100 in PBS for 2 min, and subsequently stained with 0.25 μM tetramethylrhodamine isothiocyanate (TRITC)-conjugated phalloidin (Sigma). For indirect immunofluorescence, the specimens were incubated with anti-E-cadherin antibody (BD Biosciences) and treated with Alexa546-conjugated anti-mouse IgG antibody (Invitrogen). Nuclei were visualized with 4’,6-diamidino-2-phenylindole (DAPI).

Acknowledgements

We thank Drs. Y. Endo, Y. Kido, T. Takino and H. Sato (Cancer Research Institute, Kanazawa University) for providing the cell lines and the protocol for EMT, microRNA experiments. We also thank Dr. H. Kimura (Osaka University) and Dr. N. Nozaki (Hokkaido University) for providing the antibodies that specifically recognize methylated H3K residues. This work was supported in part by Grants-in-Aid for Scientific Research from the Ministry of Education, Culture, Sports, Science and Technology of Japan.

References

1. Bannister AJ, Kouzarides T. Regulation of chromatin by histone modifications. Cell research 2011; 21:381-95.

2. Cloos PA, Christensen J, Agger K, Helin K. Erasing the methyl mark: histone demethylases at the center of cellular differentiation and disease. Genes & development 2008; 22:1115-40.

3. Mosammaparast N, Shi Y. Reversal of histone methylation: biochemical and molecular mechanisms of histone demethylases. Annual review of biochemistry 2010; 79:155-79.

4. Greer EL, Shi Y. Histone methylation: a dynamic mark in health, disease and inheritance. Nature reviews 2012; 13:343-57.

5. Kooistra SM, Helin K. Molecular mechanisms and potential functions of histone demethylases. Nat Rev Mol Cell Biol 2012; 13:297-311.

6. Bernstein BE, Kamal M, Lindblad-Toh K, Bekiranov S, Bailey DK, Huebert DJ, et al. Genomic maps and comparative analysis of histone modifications in human and

mouse. Cell 2005; 120:169-81.

7. Barski A, Cuddapah S, Cui K, Roh TY, Schones DE, Wang Z, et al. High-resolution profiling of histone methylations in the human genome. Cell 2007; 129:823-37.

8. Uren AG, Kool J, Berns A, van Lohuizen M. Retroviral insertional mutagenesis: past, present and future. Oncogene 2005; 24:7656-72.

9. Suzuki T, Shen H, Akagi K, Morse HC, Malley JD, Naiman DQ, et al. New genes involved in cancer identified by retroviral tagging. Nature genetics 2002; 32:166-74.

10. Suzuki T, Minehata K, Akagi K, Jenkins NA, Copeland NG. Tumor suppressor gene identification using retroviral insertional mutagenesis in Blm-deficient mice. The EMBO journal 2006; 25:3422-31.

11. Ishimura A, Terashima M, Kimura H, Akagi K, Suzuki Y, Sugano S, et al. Jmjd2c histone demethylase enhances the expression of Mdm2 oncogene. Biochemical and biophysical research communications 2009; 389:366-71.

12. Terashima M, Ishimura A, Yoshida M, Suzuki Y, Sugano S, Suzuki T. The tumor suppressor Rb and its related Rbl2 genes are regulated by Utx histone demethylase.

Biochemical and biophysical research communications 2010; 399:238-44.

13. Yoshida M, Ishimura A, Terashima M, Enkhbaatar Z, Nozaki N, Satou K, et al. PLU1 histone demethylase decreases the expression of KAT5 and enhances the invasive activity of the cells. The Biochemical journal 2011; 437:555-64.

14. Kalluri R, Weinberg RA. The basics of epithelial-mesenchymal transition. The Journal of clinical investigation 2009; 119:1420-8.

15. Thiery JP, Acloque H, Huang RY, Nieto MA. Epithelial-mesenchymal transitions in development and disease. Cell 2009; 139:871-90.

16. Peinado H, Olmeda D, Cano A. Snail, Zeb and bHLH factors in tumour progression: an alliance against the epithelial phenotype? Nat Rev Cancer 2007; 7:415-28.

17. Zeisberg M, Neilson EG. Biomarkers for epithelial-mesenchymal transitions. The Journal of clinical investigation 2009; 119:1429-37.

18. Miyazono K. Transforming growth factor-beta signaling in epithelial-mesenchymal transition and progression of cancer. Proceedings of the Japan Academy Series B, Physical and biological sciences 2009; 85:314-23.

19. Ke XS, Qu Y, Cheng Y, Li WC, Rotter V, Oyan AM, et al. Global profiling of

histone and DNA methylation reveals epigenetic-based regulation of gene expression during epithelial to mesenchymal transition in prostate cells. BMC genomics 2010; 11:669.

20. Wu CY, Tsai YP, Wu MZ, Teng SC, Wu KJ. Epigenetic reprogramming and post-transcriptional regulation during the epithelial-mesenchymal transition. Trends Genet 2012.

21. Lin T, Ponn A, Hu X, Law BK, Lu J. Requirement of the histone demethylase LSD1 in Snai1-mediated transcriptional repression during epithelial-mesenchymal transition. Oncogene 2010; 29:4896-904.

22. Dong C, Wu Y, Yao J, Wang Y, Yu Y, Rychahou PG, et al. G9a interacts with Snail and is critical for Snail-mediated E-cadherin repression in human breast cancer. The Journal of clinical investigation 2012; 122:1469-86.

23. Lu PJ, Sundquist K, Baeckstrom D, Poulsom R, Hanby A, Meier-Ewert S, et al. A novel gene (PLU-1) containing highly conserved putative DNA/chromatin binding motifs is specifically up-regulated in breast cancer. The Journal of biological chemistry 1999; 274:15633-45.

24. Xiang Y, Zhu Z, Han G, Ye X, Xu B, Peng Z, et al. JARID1B is a histone H3

lysine 4 demethylase up-regulated in prostate cancer. Proceedings of the National Academy of Sciences of the United States of America 2007; 104:19226-31.

25. Yamane K, Tateishi K, Klose RJ, Fang J, Fabrizio LA, Erdjument-Bromage H, et al. PLU-1 is an H3K4 demethylase involved in transcriptional repression and breast cancer cell proliferation. Molecular cell 2007; 25:801-12.

26. Hayami S, Yoshimatsu M, Veerakumarasivam A, Unoki M, Iwai Y, Tsunoda T, et al. Overexpression of the JmjC histone demethylase KDM5B in human carcinogenesis: involvement in the proliferation of cancer cells through the E2F/RB pathway. Molecular cancer 2010; 9:59.

27. Ishimura A, Minehata K, Terashima M, Kondoh G, Hara T, Suzuki T. Jmjd5, an H3K36me2 histone demethylase, modulates embryonic cell proliferation through the regulation of Cdkn1a expression. Development 2012; 139:749-59.

28. Kimura H, Hayashi-Takanaka Y, Goto Y, Takizawa N, Nozaki N. The organization of histone H3 modifications as revealed by a panel of specific monoclonal antibodies. Cell structure and function 2008; 33:61-73.

29. Kasai H, Allen JT, Mason RM, Kamimura T, Zhang Z. TGF-beta1 induces

human alveolar epithelial to mesenchymal cell transition (EMT). Respiratory research 2005; 6:56.

30. Gregory PA, Bert AG, Paterson EL, Barry SC, Tsykin A, Farshid G, et al. The miR-200 family and miR-205 regulate epithelial to mesenchymal transition by targeting ZEB1 and SIP1. Nature cell biology 2008; 10:593-601.

31. Park SM, Gaur AB, Lengyel E, Peter ME. The miR-200 family determines the epithelial phenotype of cancer cells by targeting the E-cadherin repressors ZEB1 and ZEB2. Genes & development 2008; 22:894-907.

32. Bracken CP, Gregory PA, Kolesnikoff N, Bert AG, Wang J, Shannon MF, et al. A double-negative feedback loop between ZEB1-SIP1 and the microRNA-200 family regulates epithelial-mesenchymal transition. Cancer research 2008; 68:7846-54.

33. Davalos V, Moutinho C, Villanueva A, Boque R, Silva P, Carneiro F, et al. Dynamic epigenetic regulation of the microRNA-200 family mediates epithelial and mesenchymal transitions in human tumorigenesis. Oncogene 2011; 31:2062-74.

34. Kahl P, Gullotti L, Heukamp LC, Wolf S, Friedrichs N, Vorreuther R, et al. Androgen receptor coactivators lysine-specific histone demethylase 1 and four and a half

LIM domain protein 2 predict risk of prostate cancer recurrence. Cancer research 2006; 66:11341-7.

35. Chase A, Cross NC. Aberrations of EZH2 in cancer. Clin Cancer Res 2011; 17:2613-8.

36. Lv T, Yuan D, Miao X, Lv Y, Zhan P, Shen X, et al. Over-expression of LSD1 promotes proliferation, migration and invasion in non-small cell lung cancer. PloS one 2012; 7:e35065.

37. Hayami S, Kelly JD, Cho HS, Yoshimatsu M, Unoki M, Tsunoda T, et al. Overexpression of LSD1 contributes to human carcinogenesis through chromatin regulation in various cancers. International journal of cancer 2011; 128:574-86.

38. Vrba L, Jensen TJ, Garbe JC, Heimark RL, Cress AE, Dickinson S, et al. Role for DNA methylation in the regulation of miR-200c and miR-141 expression in normal and cancer cells. PloS one 2010; 5:e8697.

39. Cao Q, Mani RS, Ateeq B, Dhanasekaran SM, Asangani IA, Prensner JR, et al. Coordinated regulation of polycomb group complexes through microRNAs in cancer. Cancer cell 2011; 20:187-99.

40. Pereira F, Barbachano A, Singh PK, Campbell MJ, Munoz A, Larriba MJ. Vitamin D has wide regulatory effects on histone demethylase genes. Cell Cycle 2012; 11:1081-9.

Figure legends

Figure 1. Overexpression of KDM5B caused morphological changes of A549 cells.

(A) Cell morphological changes of A549 cells induced by KDM5B. A549 cells infected with the control retrovirus, the control retrovirus with TGF-β treatment, or the retrovirus expressing FLAG-tagged wild-type (WT) KDM5B or the H499Y mutant (Mut), were stained with crystal violet. (B) Immunofluorescence images of cells showing the localization of E-cadherin. The panels of A549 cells with the same arrangement with (A) were stained with anti-E-cadherin antibody and with DAPI. (C) Fluorescence images of cells showing reorganization of actin cytoskeleton. The cells were stained with TRITC-phalloidin (indicated as Actin) and with DAPI.

Figure 2. KDM5B affected the expression of EMT-related genes.

Quantitative RT-PCR analysis was performed to detect the expression of *CDH1/E-cadherin* (A), *FN1/Fibronectin* (B), *CDH2/N-cadherin* (C), *SNAI1* (D), *SNAI2* (E), *ZEB1* (F) and *ZEB2* (G) in A549 cells infected with the control retrovirus, the control retrovirus with TGF-β treatment, or the retrovirus expressing wild-type (WT) KDM5B or the mutant (Mut). PCR data were normalized with respect to control human *GAPDH* expression. The averages from at least three experiments are presented with the standard deviations (∗, $P <$ 0.001 comparing to control). (H) Western blotting was performed to detect the expression of E-cadherin, ZEB1 and ZEB2 proteins using the corresponding antibodies. As a control, anti-GAPDH antibody was used to show that equal amounts of proteins were loaded on the gel.

Figure 3. Recruitment of KDM5B was not detected on the regulatory regions of *CDH1/E-cadherin*, *ZEB1* and *ZEB2* genes.

Schematic of the regulatory regions of *CDH1/E-cadherin* (A), *ZEB1* (C) and *ZEB2* genes (E) is presented. The boxes shown on the scheme indicate the first and second exons and the dark area corresponds to the coding region. The arrow points to the transcription initiation site. The regions covered by the primer sets used for ChIP assays are shown as a. ChIP analyses of H3K4me3, H3K27me3 and FLAG-tagged KDM5B on the regulatory regions of *CDH1/E-cadherin* (B), *ZEB1* (D) and *ZEB2* genes (F) are shown. Cross-linked chromatins from A549 cells infected with the control retrovirus or the retrovirus expressing wild-type KDM5B were immunoprecipitated with the specific antibodies. The occupancies of methylated histones or KDM5B protein on the regions were analyzed by quantitative PCR and presented as the percentages of enrichment over input DNA. The averages from at least three experiments are presented with the standard deviations (∗, $P < 0.001$ comparing to control; **, $P < 0.05$ comparing to control).

Figure 4. KDM5B decreased the expression of miR-200a and miR-200c by converting the histone H3 methylation on the regulatory regions of miR-200 gene clusters.

Quantitative RT-PCR analysis was performed to detect the expression of miR-200a (A), and miR-200c (B) in A549 cells infected with the control retrovirus, the control retrovirus with TGF-β treatment, or the retrovirus expressing wild-type (WT) KDM5B or the mutant (Mut). PCR data were normalized with respect to control human *RNU6B* expression (∗, $P <$ 0.001 comparing to control). Schematic representation of the regulatory regions of *miR-200b/200a/429* (C) and *miR-200c/141* genes (E) is shown. The regions covered by the primer sets used for ChIP assays are shown as a and b. ChIP analyses of H3K4me3, H3K27me3 and FLAG-tagged KDM5B on the regulatory regions of *miR-200b/200a/429* (D) and *miR-200c/141* genes (F) are shown (∗, $P <$ 0.001 comparing to control; **, $P <$ 0.005 comparing to control).

Figure 5. Altered expression of EMT-related gene induced by KDM5B was cancelled with the introduction of exogenous miR-200.

Quantitative RT-PCR analysis was performed to detect the expression of *CDH1/E-cadherin* (A), *CDH2/N-cadherin* (B), *ZEB1* (C) and *ZEB2* (D) in A549 cells infected with the control retrovirus, the retrovirus expressing wild-type KDM5B, KDM5B with miR-200a precursor and KDM5B with miR-200c precursor (∗, $P < 0.001$ comparing to KDM5B WT).

Figure 6. Knockdown of KDM5B affected the expression of EMT-related genes in A549 cells.

Quantitative RT-PCR analysis was performed to detect the expression of *CDH1* (A), *FN1* (B), *CDH2* (C), *ZEB1* (D) and *ZEB2* (E) in A549 cells expressing control shRNA or KDM5B shRNA (∗, $P < 0.001$ comparing to control; **, $P < 0.005$ comparing to control). (F) Western blotting was performed to detect the expression of E-cadherin, ZEB1 and ZEB2 proteins using the corresponding antibodies. Quantitative RT-PCR for miR-200a (G) and miR-200c (H) was performed (∗, $P < 0.001$ comparing to control; **, $P < 0.005$ comparing to control). (I, J) ChIP analysis of H3K4me3 and H3K27me3 on the regulatory regions a of *miR-200b/200a/429* (I) and *miR-200c/141* genes (J) in A549 cells expressing control shRNA or KDM5B shRNA (∗, $P < 0.001$ comparing to control; **, $P < 0.005$ comparing to control; ***, $P < 0.01$ comparing to control).

Figure 7. Significant association between *KDM5B* and *ZEB* family expressions in human lung cancer samples.

Quantitative RT-PCR analysis was performed to detect the expression of *KDM5B*, *ZEB1* and *ZEB2* in human lung cancer tissues (N=24). PCR data were normalized with respect to control human *DDX5* expression. Association of *KDM5B* and *ZEB1* expression (A) or *KDM5B* and *ZEB2* expression (B) was estimated using Pearson correlation coefficient. The associations were significantly positive with r=0.442 ($P < 0.05$) and with r=0.601 ($P < 0.005$), respectively.

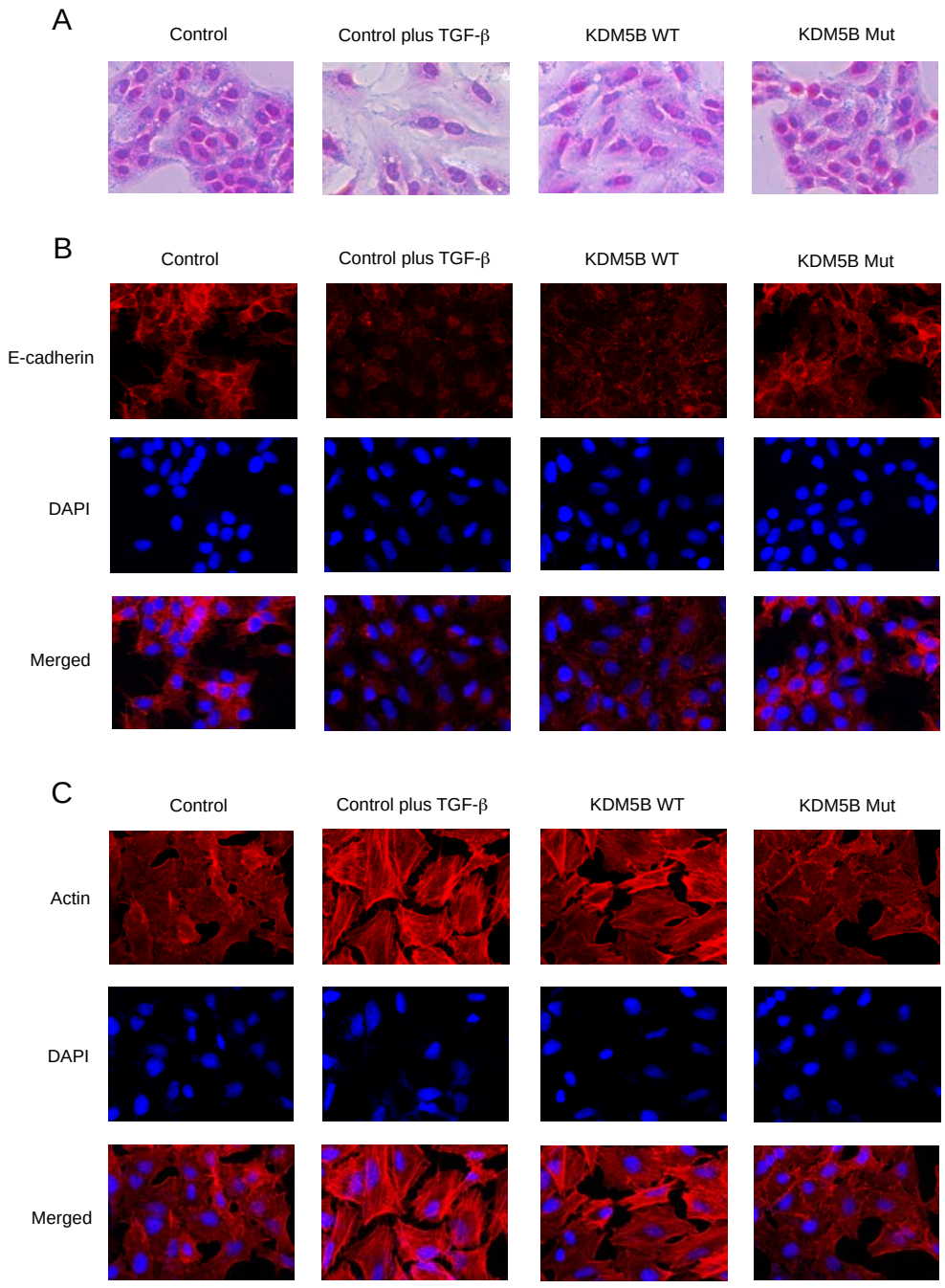

Enkhbaatar et al. Figure 1

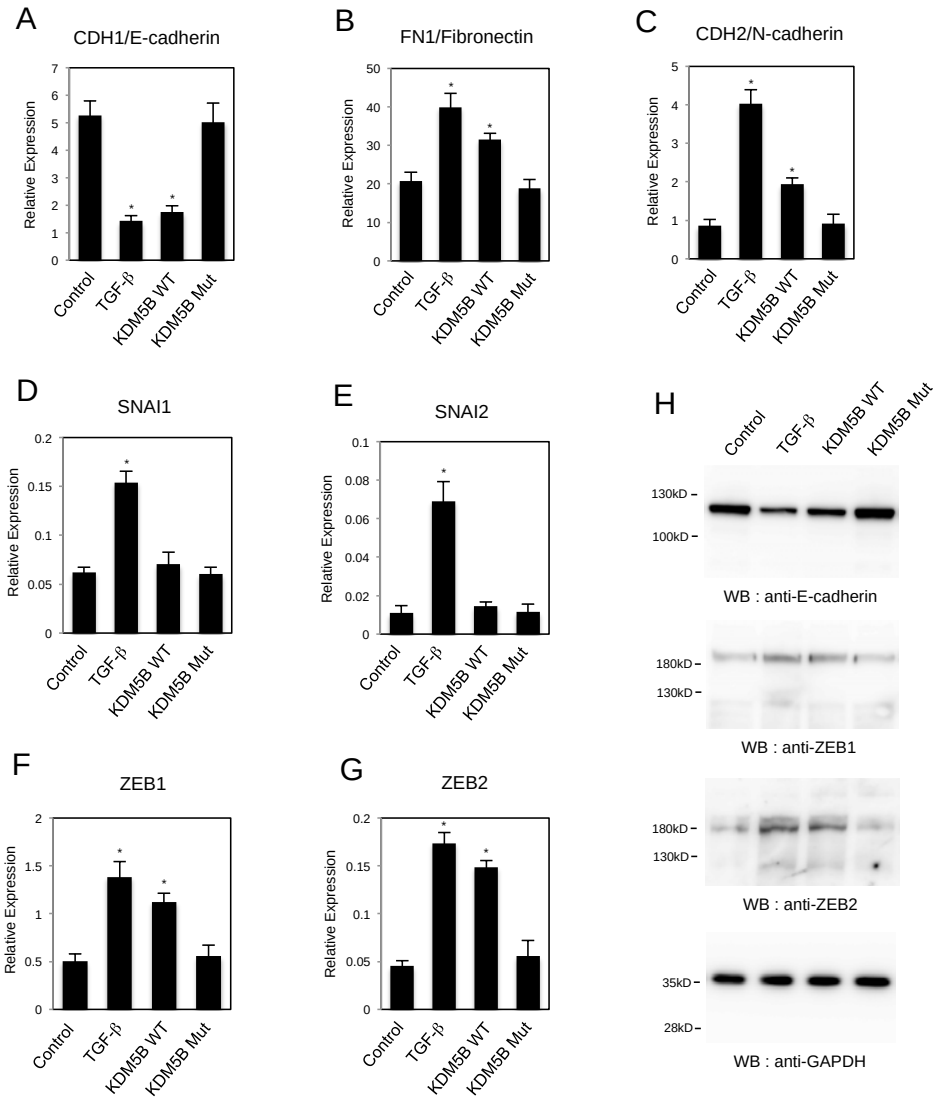

Enkhbaatar et al. Figure 2

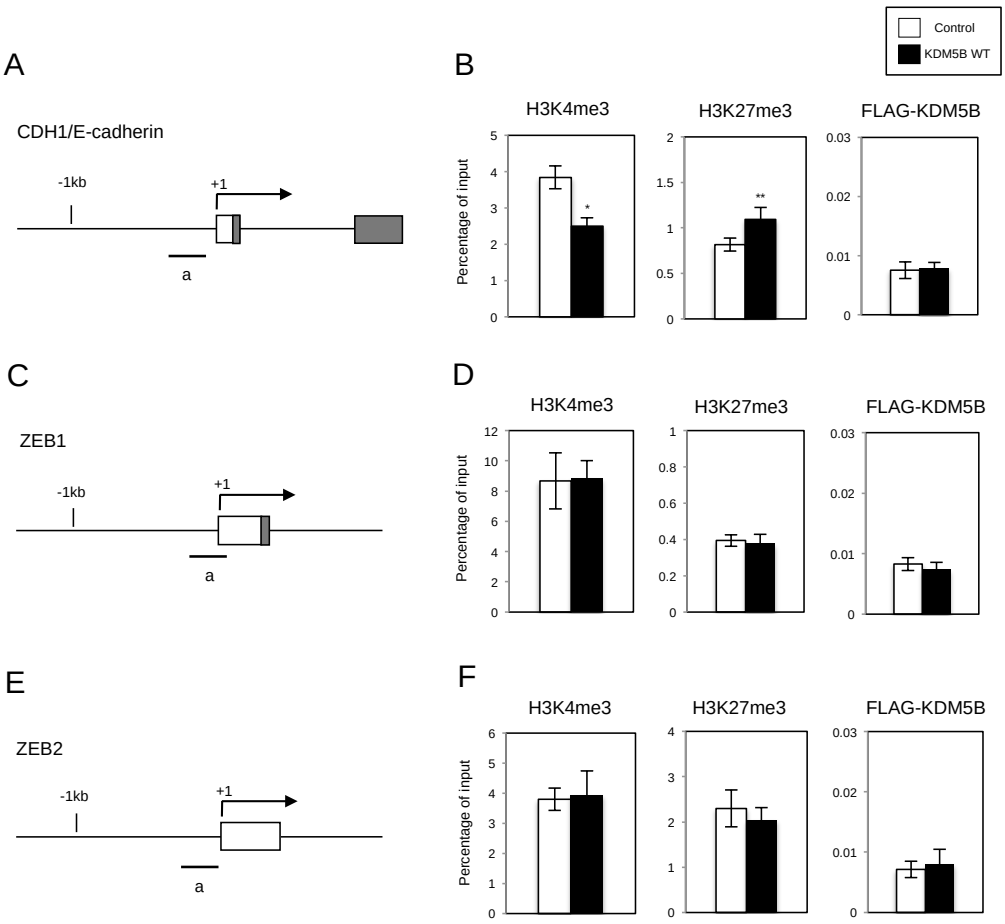

Enkhbaatar et al. Figure 3

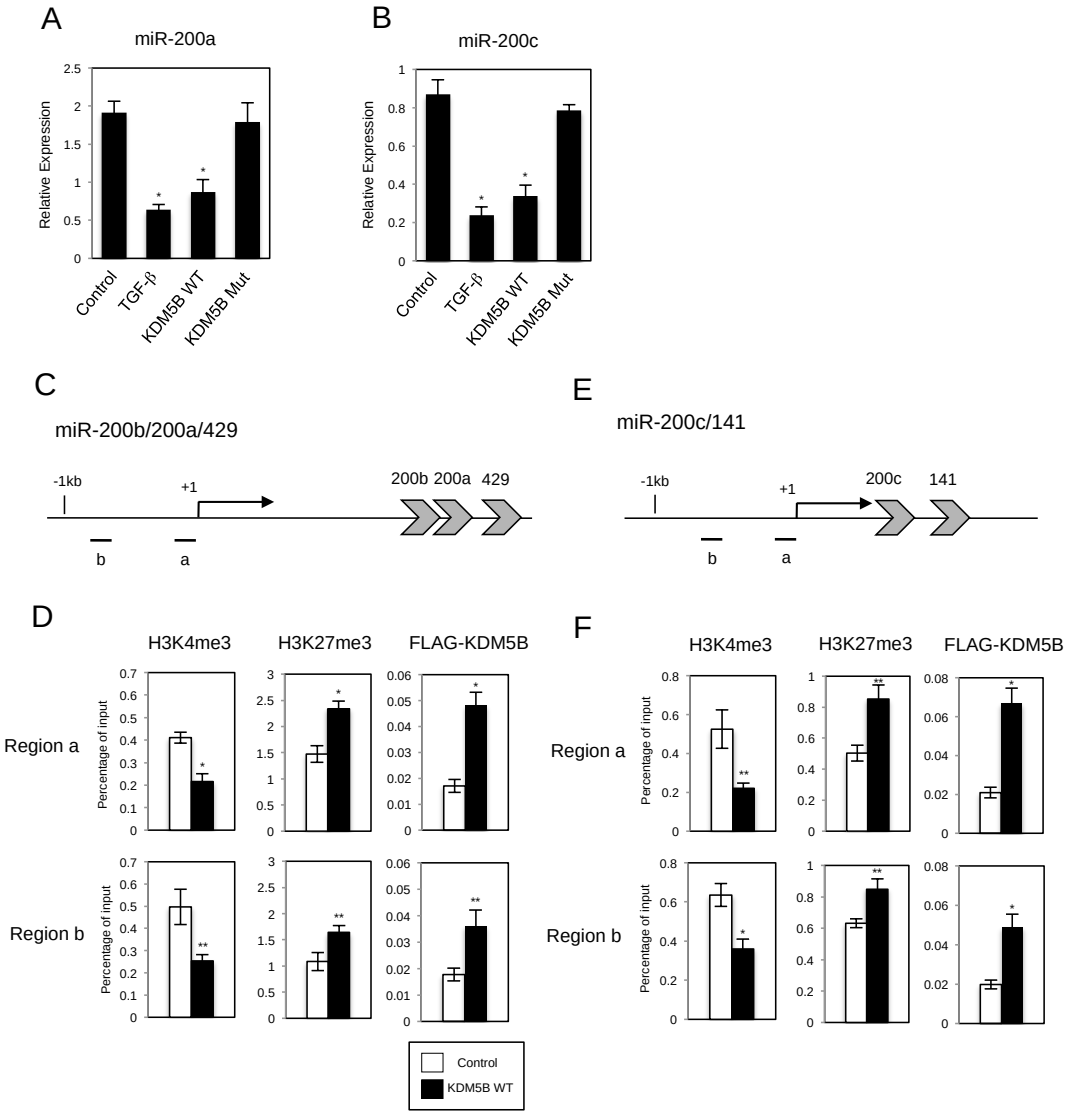

Enkhbaatar et al. Figure 4

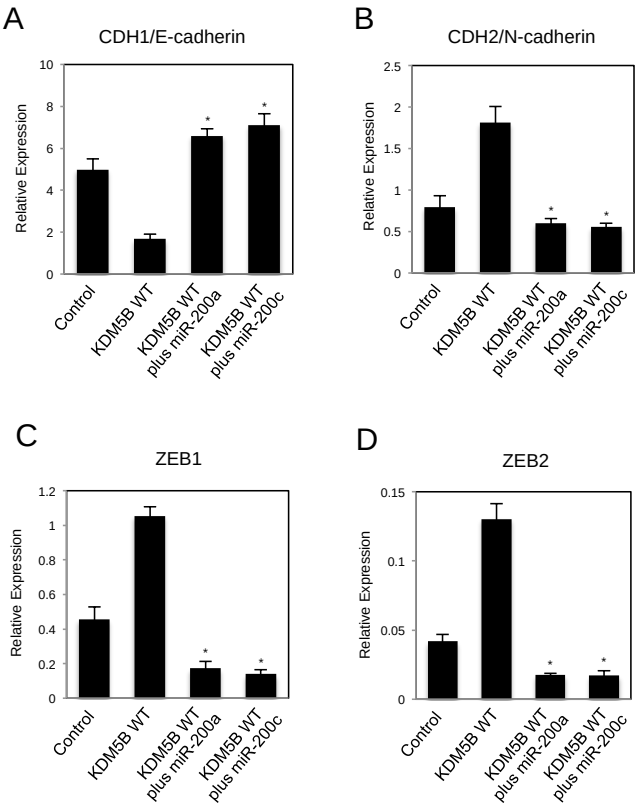

Enkhbaatar et al. Figure 5

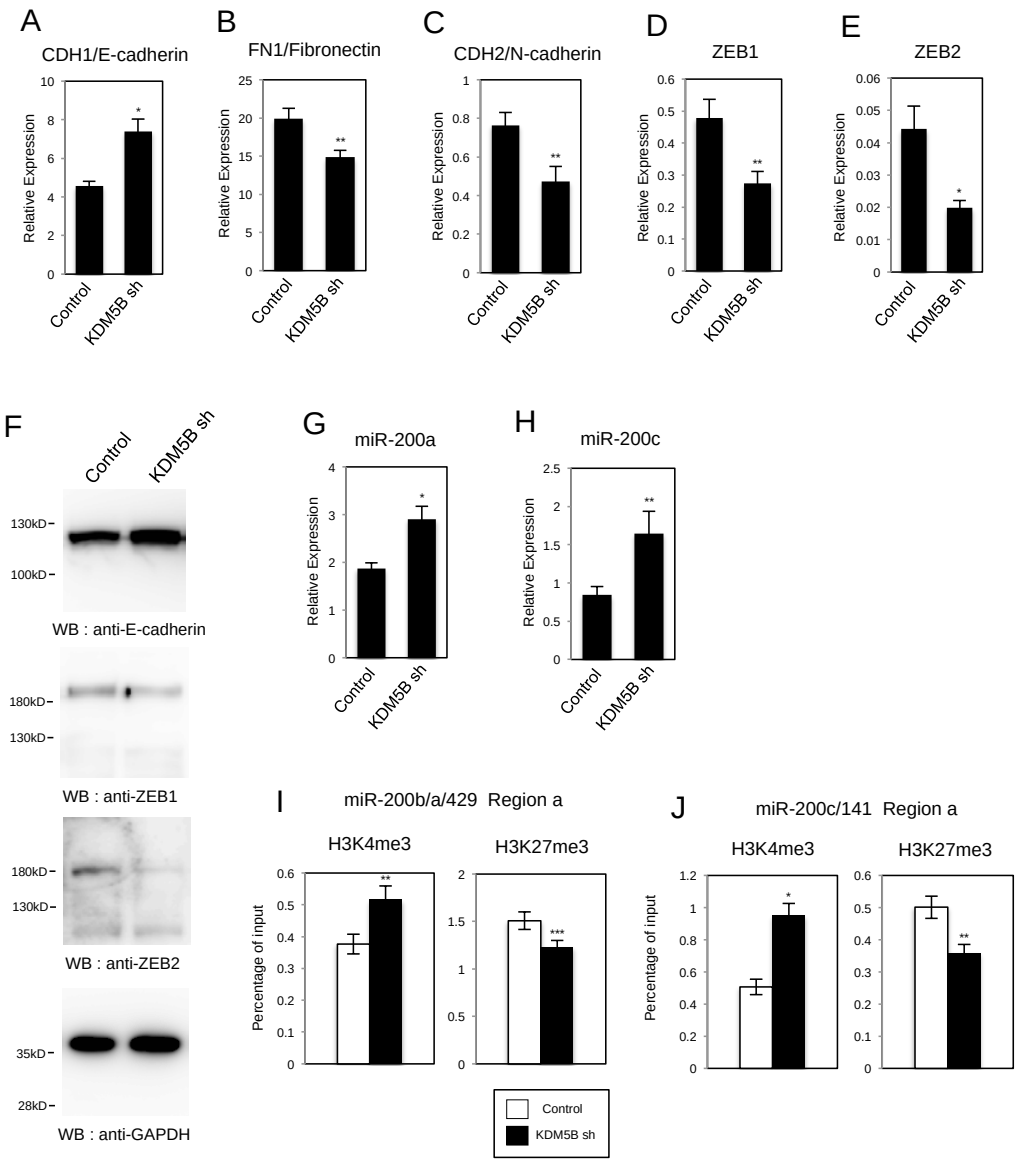

Enkhbaatar et al. Figure 6

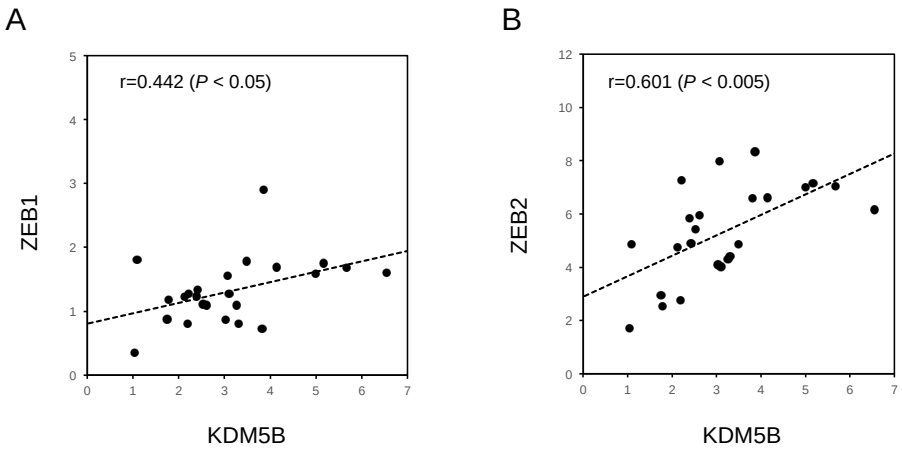

Enkhbaatar et al. Figure 7

Table S1 Quantitative PCR primers used in this study

Gene	**Primer sequence (5’ to 3’)**
CDH1/E-cadherin	F: tgcccagaaaatgaaaaagg R: gtgtatgtggcaatgcgttc
FN1/Fibronectin	F: cagtgggagacctcgagaag R: tccctcggaacatcagaaac
CDH2/N-cadherin	F: acagtggccacctacaaagg R: ccgagatggggttgataatg
SNAI1	F: accccaatcggaagcctaact R: agatgagcattggcagcga
SNAI2	F: gcctccaaaaagccaaactaca R: gctgaggatctctggttgtggt
ZEB1	F: ttcaaacccatagtggttgct R: tgggagataccaaaccaactg
ZEB2	F: caagaggcgcaaacaagc R: ggttggcaataccgtcatcc
DDX5	F: tatggttggagtggcacaga R: ccagcaccaaacaaataggc
Mouse *Cdh1/E-cadherin*	F: aggagaacggtggtcaaaga R: gctggctcaaatcaaagtcc
Mouse *Fn1/Fibronectin*	F: ggaatggacctgcaaacctat R: catcatccagccttggtagg
Mouse *Cdh2/N-cadherin*	F: cattatcaaccccatctcagg R: tgcatgtgctctcaagtgaa
Mouse *Snai1*	F: cttgtgtctgcacgacctgt R: caggagaatggcttctcacc
Mouse *Snai2*	F: ctcacctcgggagcatacagc R: tgaagtgtcagaggaaggcggg
Mouse *Zeb1*	F: ttcaaacccatagtggttgct R: tgggagataccaaaccaactg
Mouse *Zeb2*	F: atgagcttcctaccgcatatgg R: tgtagtcttgtgctccatccag
Mouse *Actb/beta-Actin*	F: gctgtattcccctccatcgtg R: cacggttggccttagggttcag
CDH1 gene region g	F: aactactgttggggctgggt R: ggtgctaactgataggggtg
CDH1 gene region f	F: gatgttaggaaagcaatggg R: gtaaatgctgtccagggct
CDH1 gene region e	F: gaaacagagaagcaattcagtg R: cagtagatcaggtgtccaggg
CDH1 gene region d	F: ggctagtgagtggctgactc R: acaacttccctgtctgactcc
CDH1 gene region c	F: agtgagccaagaacacacca

	R: tgtgccagtctctgtgctaag
CDH1 gene region b	F: aaggcaggaggatcgcttc R: tgtagagagacaagtcggggc
CDH1 gene region a	F: ttctgatcccaggtcttagtg R: gttgctagggtctaggtgggtta
CDH1 gene region h	F: ggataagaaagtgaggtcgg R: gatgtctttattctccagtaccc
CDH1 gene region i	F: caaaccgaggctaagagagtg R: cagagatggtgcttaatggg
CDH1 gene region j	F: gctttgttccacttgactgtt R: gcctcttattgtgataccca
ZEB1 gene region g	F: ccattctgtggtaaactatgtaac R: gtgatgcagaacccacagtt
ZEB1 gene region f	F: gtatcccctaccgtttgattt R: atacagctaaagaataggggaa
ZEB1 gene region e	F: tctatgacctgattcggtag R: tatgtcaacacggtgtccttg
ZEB1 gene region d	F: acttctagcctctctttcaatcc R: agagaggctacctgacccg
ZEB1 gene region c	F: gaaagtagtgctctctgccc R: agaccaggtaagagacataacg
ZEB1 gene region b	F: gctgctgtgccaagggaaa R: aggcgactgtgcaaccacc
ZEB1 gene region a	F: gctttggttcctgcgttattt R: ttctcctaaacacgtatttcctcg
ZEB1 gene region h	F: cagcaaatggcaacttgtg R: aatgaaagcagcagacagga
ZEB1 gene region i	F: tggaatatgtctgaaggtagga R: accacacaaggtttgatgct
ZEB1 gene region j	F: gagggctcagtagtgaatagg R: ctccatgctacaatgtatctcg
ZEB2 gene region e	F: ttggagtaagttggatgcgac R: tggttttcaattccctggtg
ZEB2 gene region d	F: ttcctcaactttcacagccg R: ctgtgtgttcaagggcagaaa
ZEB2 gene region c	F: ctttacagccacccttccac R: ggtctgtaagcctccaatgg
ZEB2 gene region b	F: gtgttcttaaccaatgctctgct R: cctgtgctcagcatcctca
ZEB2 gene region a	F: cctttggcatcattatcctcat R: actttcgccccttggagttc
ZEB2 gene region f	F: aaacctacctgcgaagtcttgtt R: cgacactcttggcgaggttt
ZEB2 gene region g	F: tgcctgttactcctaagtctg R: ccaggaacagtgatgagcc
ZEB2 gene region h	F: ggagtttatcgaggcactgtc

	R: gacagtgtccaaagaggctta
ZEB2 gene region i	F: ggaaaagtttggttcgggc R: cttatcaatgaagcagccgat
ZEB2 gene region j	F: gagcgagaagtttccttcc R: tgacggaggataactgagttt
miR-200b/a/429 gene region a	F: tatgggagcccaggggaca R: ctcgccttacaaggagcagtg
miR-200b/a/429 gene region b	F: gctgtgggtctgtggggtct R: tttggagcaatgaagggacc
miR-200c/141 gene region a	F: agggctcaccaggaagtgt R: ttgggtcaggcagcttcag
miR-200c/141 gene region b	F: gaaggggttaaggcagtgg R: cctccgctcttcctcctt
GAPDH gene region a	F: tactagcggttttacgggcg R: gaggctgcgggctcaattt
GAPDH gene region b	F: atcgtgaccttccgtgcaga R: catctcctggctcctggcat
BRCA1 gene region a	F: aatcagaggatgggaggga R: ctttatggcaaactcaggtagaa
BRCA1 gene region b	F: agtagtcttgtaaggtcagtggc R: taacaaacactggggctgag
HOXA5 gene region a	F: tgtgtgcttgatttgtggct R: cgtaggagggaaccaagtacat
HOXA5 gene region b	F: tgtgtagtgtttctccaaggc R: aaatcgcaaactaatgacacg

F: Forward, R: Reverse

Supplementary Figure legends

Figure 1. Expression of KDM5B proteins in the cells infected with the retroviruses.
A549 cells (A), NMuMG cells (B) or HT29 cells (C) were infected with the control retrovirus or the retrovirus expressing FLAG-tagged wild-type (WT) KDM5B or the H499Y mutant (Mut). KDM5B proteins were detected by Western blot (WB) with anti-FLAG antibody (upper panel). As a loading control, anti-GAPDH antibody was used (lower panel).

Figure 2. Overexpression of KDM5B caused morphological changes of NMuMG mouse breast epithelial cells.
(A) Cell morphological changes of NMuMG cells induced by KDM5B. NMuMG cells infected with the control retrovirus, the control retrovirus with TGF-β treatment, or the retrovirus expressing FLAG-tagged wild-type (WT) KDM5B or the H499Y mutant (Mut), were stained with crystal violet. (B) Immunofluorescence images of cells showing the localization of E-cadherin. The panels of NMuMG cells with the same arrangement with (A) were stained with anti-E-cadherin antibody and with DAPI. (C) Fluorescence images of cells showing reorganization of actin cytoskeleton. The cells were stained with TRITC-phalloidin (indicated as Actin) and with DAPI.

Figure 3. Overexpression of KDM5B caused morphological changes of HT29 human colon cancer cells.
(A) Cell morphological changes of HT29 cells induced by KDM5B. HT29 cells infected with the control retrovirus, the control retrovirus with TGF-β treatment, or the retrovirus expressing FLAG-tagged wild-type (WT) KDM5B or the H499Y mutant (Mut), were stained with crystal violet. (B) Immunofluorescence images of cells showing the localization of E-cadherin. The panels of HT29 cells with the same arrangement with (A) were stained with anti-E-cadherin antibody and with DAPI. (C) Fluorescence images of cells showing reorganization of actin cytoskeleton. The cells were stained with TRITC-phalloidin (indicated as Actin) and with DAPI.

Figure 4. KDM5B affected the expression of EMT-related genes in NMuMG cells.
Quantitative RT-PCR analysis was performed to detect the expression of mouse *CDH1/E-cadherin* (A), *FN1/ Fibronectin* (B), *CDH2/N-cadherin* (C), *SNAI1* (D), *SNAI2* (E), *ZEB1* (F) and *ZEB2* (G) in NMuMG cells infected with the control retrovirus, the control retrovirus with TGF-β treatment, or the retrovirus expressing wild-type (WT) KDM5B or the mutant (Mut). PCR data were normalized with respect to control mouse *Actb* expression (*, $P < 0.001$ comparing to control; **, $P < 0.005$ comparing to control). (H) Western blot analysis was performed to detect the expression of E-cadherin and ZEB1 proteins using the corresponding antibodies.

Figure 5. KDM5B affected the expression of EMT-related genes in HT29 cells.
Quantitative RT-PCR analysis was performed to detect the expression of human *CDH1/E-cadherin* (A), *FN1/ Fibronectin* (B), *SNAI1*(C) and *ZEB1* (D) in HT29 cells infected with the control retrovirus, the control retrovirus with TGF-β treatment, or the retrovirus expressing wild-type (WT) KDM5B or the mutant (Mut). The expression levels of *CDH2/N-cadherin, SNAI2* and *ZEB2* were extremely low or not detected in HT29 cells. PCR data were normalized with respect to control *GAPDH* expression (*, $P < 0.001$ comparing to control; **, $P < 0.005$ comparing to control). (E) Western blot analysis was performed to detect the expression of E-cadherin and ZEB1 proteins using the corresponding antibodies.

Figure 6. Recruitment of KDM5B was not detected on the various regions upstream or around the transcription initiation site of *CDH1/E-cadherin* gene.
(A) Schematic representation of the regions upstream or around the transcription initiation site of *CDH1/E-cadherin* gene. The boxes shown on the scheme indicate the first and second exons and the dark area corresponds to the coding region. The arrow points to the transcription initiation site. The regions covered by the primer sets used for ChIP assays are shown as a to j. (B) ChIP analyses of H3K4me3, H3K27me3 and FLAG-tagged KDM5B on the regulatory regions. The occupancies of methylated histones or KDM5B protein on the regions were analyzed by quantitative PCR and presented as the percentages of enrichment over input DNA (*, $P < 0.01$ comparing to control; **, $P < 0.05$ comparing to control).

Figure 7. Recruitment of KDM5B was not detected on the various regions upstream or around the transcription initiation site of *ZEB1* gene.
(A) Schematic representation of the regions upstream or around the transcription initiation site of *ZEB1* gene. The regions covered by the primer sets used for ChIP assays are shown as a to j. (B) ChIP analyses of H3K4me3, H3K27me3 and FLAG-tagged KDM5B on the regulatory regions. The occupancies of methylated histones or KDM5B protein on the regions were analyzed by quantitative PCR and presented as the percentages of enrichment over input DNA

Figure 8. Recruitment of KDM5B was not detected on the various regions upstream or around the transcription initiation site of *ZEB2* gene.
(A) Schematic representation of the regions upstream or around the transcription initiation site of *ZEB2* gene. The regions covered by the primer sets used for ChIP assays are shown as a to j. (B) ChIP analyses of H3K4me3, H3K27me3 and FLAG-tagged KDM5B on the regulatory regions. The occupancies of methylated histones or KDM5B protein on the regions were analyzed by quantitative PCR and presented as the percentages of enrichment over input DNA.

Figure 9. KDM5B decreased the expression of miR-200a and miR-200c both in NMuMG and HT29 cells.
Quantitative RT-PCR analysis was performed to detect the expression of miR-200a, and miR-200c in NMuMG cells (A and B) and HT29 cells (C and D) infected with the control retrovirus, the control retrovirus with TGF-β treatment, or the retrovirus expressing wild-type (WT) KDM5B or the mutant (Mut). PCR data were normalized with respect to control mouse *snoRNA202* or human *U6B* expression (*, $P < 0.001$ comparing to control; **, $P < 0.005$ comparing to control).

Figure 10. ChIP experiments for the regulatory regions of *BRCA1, HOXA5* and *GAPDH* genes.
Schematic of the regulatory regions of *BRCA1* (A), *HOXA5* (C) and *GAPDH* (E) genes is presented. The boxes shown on the scheme indicate the first and second exons and the dark area corresponds to the coding region. The arrow points to the transcription initiation site. The regions covered by the primer sets used for ChIP assays are shown as a and b. ChIP analyses of H3K4me3, H3K27me3 and FLAG-tagged KDM5B on the regulatory regions of *BRCA1* (B), *HOXA5* (D) and *GAPDH* (F) genes are shown. The occupancies of methylated histones or KDM5B protein on the regions were analyzed by quantitative PCR and presented as the percentages of enrichment over input DNA (*, $P < 0.001$ comparing to control; **, $P < 0.005$ comparing to control).

Figure 11. KDM5B-induced EMT phenotype was inhibited with the introduction of exogenous miR-200.
(A) Immunofluorescence images of cells showing the localization of E-cadherin. A549 cells infected with the control retrovirus, the retrovirus expressing wild-type KDM5B, KDM5B with miR-200a precursor and KDM5B with miR-200c precursor were stained with anti-E-cadherin antibody and with DAPI. (B) Fluorescence images of cells showing reorganization of actin cytoskeleton. The panels of A549 cells with the same arrangement with (A) were stained with TRITC-phalloidin (indicated as Actin) and with DAPI.

Figure 12. Introduction of exogenous miRNA-200 precursor did not affect the expression level of KDM5B protein.
Western blot with anti-FLAG antibody was performed to detect KDM5B proteins in A549 cells infected with the retrovirus expressing FLAG-tagged wild-type (WT) KDM5B, KDM5B with miR-200a precursor and KDM5B with miR-200c precursor. As a loading control, anti-GAPDH antibody was used.

Figure 13. Knockdown of KDM5B affected the E-cadherin expression in A549 cells but did not counteract with TGF-β-induced EMT phenotype.
(A) Immunofluorescence images of cells showing the localization of E-cadherin. A549 cells were infected with retroviruses expressing control shRNA or KDM5B shRNA with or without treatment of TGF-β, and were stained with anti-E-cadherin antibody and with DAPI. (B) Fluorescence images of cells showing reorganization of actin cytoskeleton. The panels of A549 cells with the same arrangement with (A) were stained with TRITC-phalloidin (indicated as Actin) and with DAPI.

Figure 14. Knockdown of KDM5B did not affect TGF-β-induced expression changes of EMT-related genes.
Quantitative RT-PCR analysis was performed to detect the expression of *CDH1/E-cadherin* (A), *FN1/Fibronectin* (B), *CDH2/N-cadherin* (C), *ZEB1* (D) and *ZEB2* (E) in A549 cells infected with retroviruses expressing control shRNA or KDM5B shRNA with or without treatment of TGF-β (*, $P < 0.001$ comparing to control).

Figure 15. The expression of endogenous KDM5B is slightly induced by the treatment of TGF-β in A549 cells.
Quantitative RT-PCR analysis was performed to detect the expression of *KDM5B* in A549 cells before and after TGF-β treatment (12h, 24h and 48h) (*, $P < 0.001$ comparing to control; **, $P < 0.01$ comparing to control).

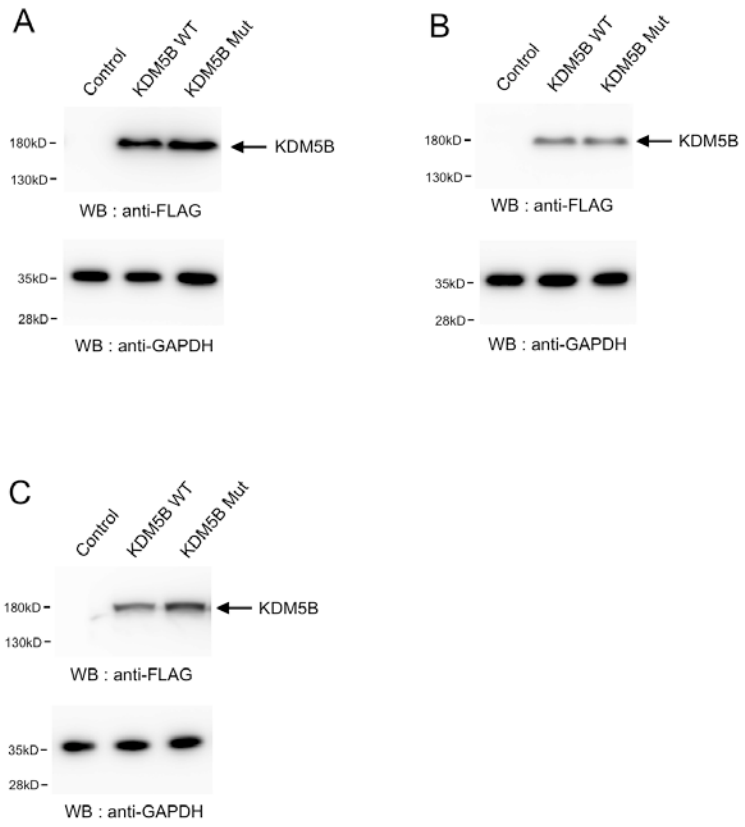

Enkhbaatar et al. Supplementary Figure 1

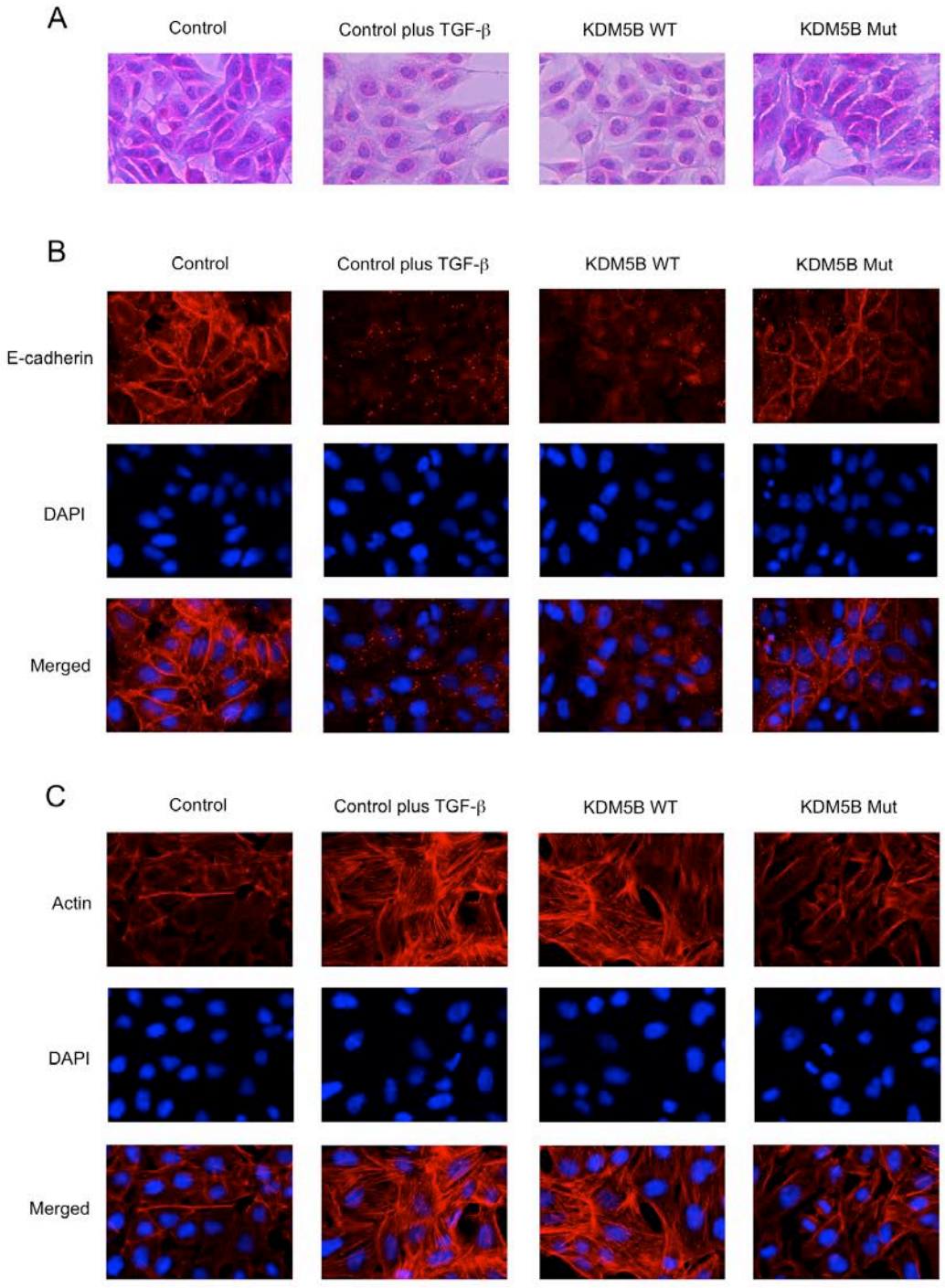

Enkhbaatar et al. Supplementary Figure 2

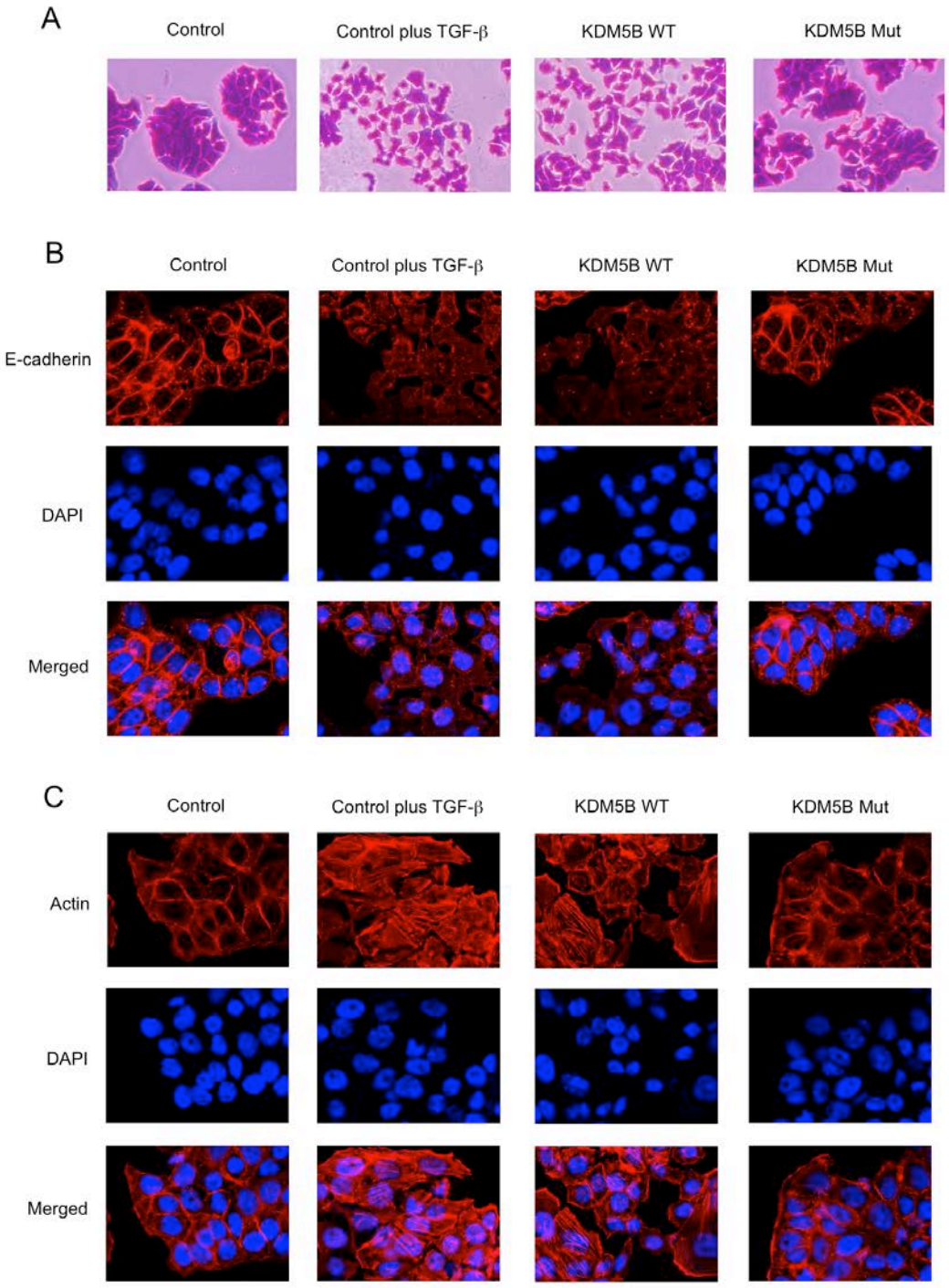

Enkhbaatar et al. Supplementary Figure 3

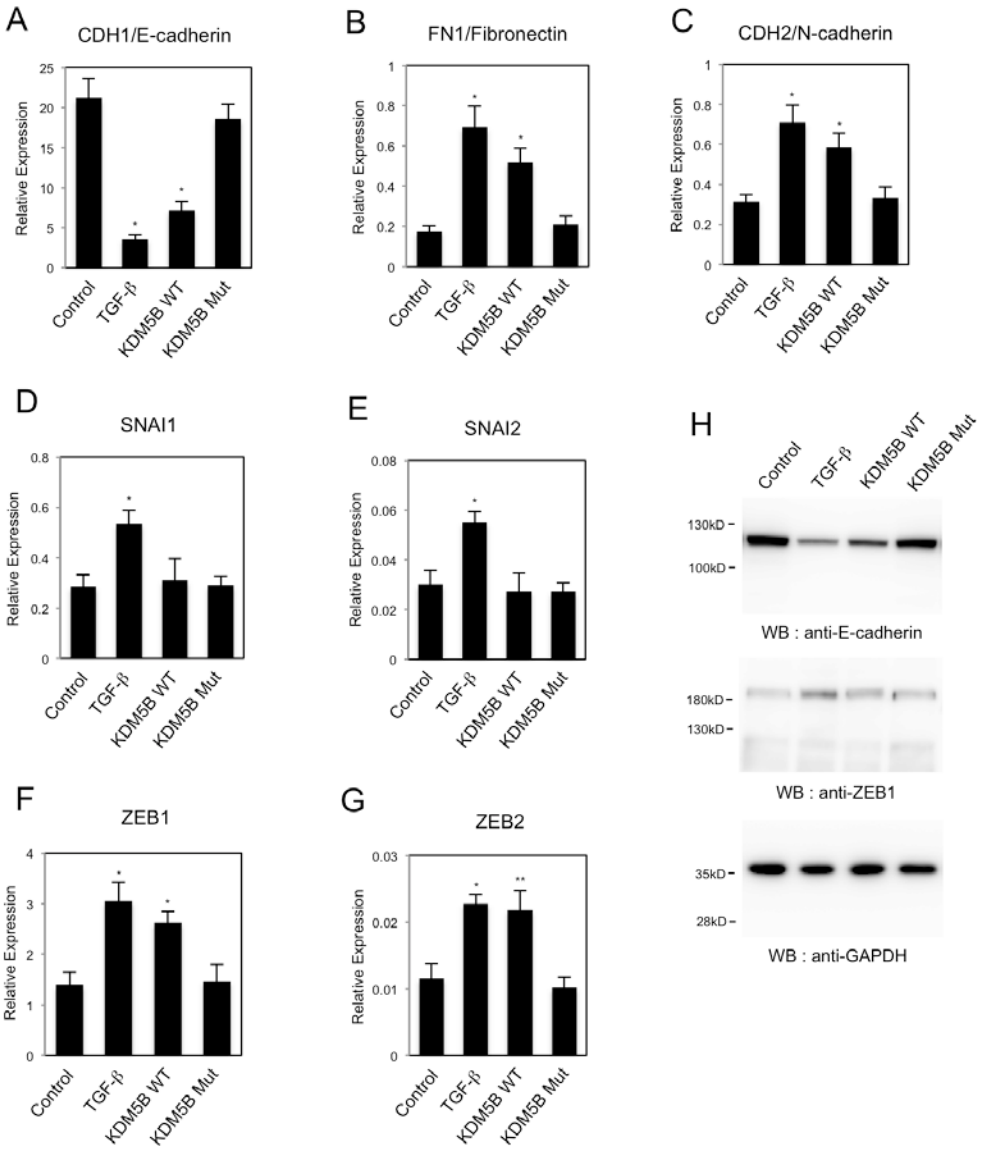

Enkhbaatar et al. Supplementary Figure 4

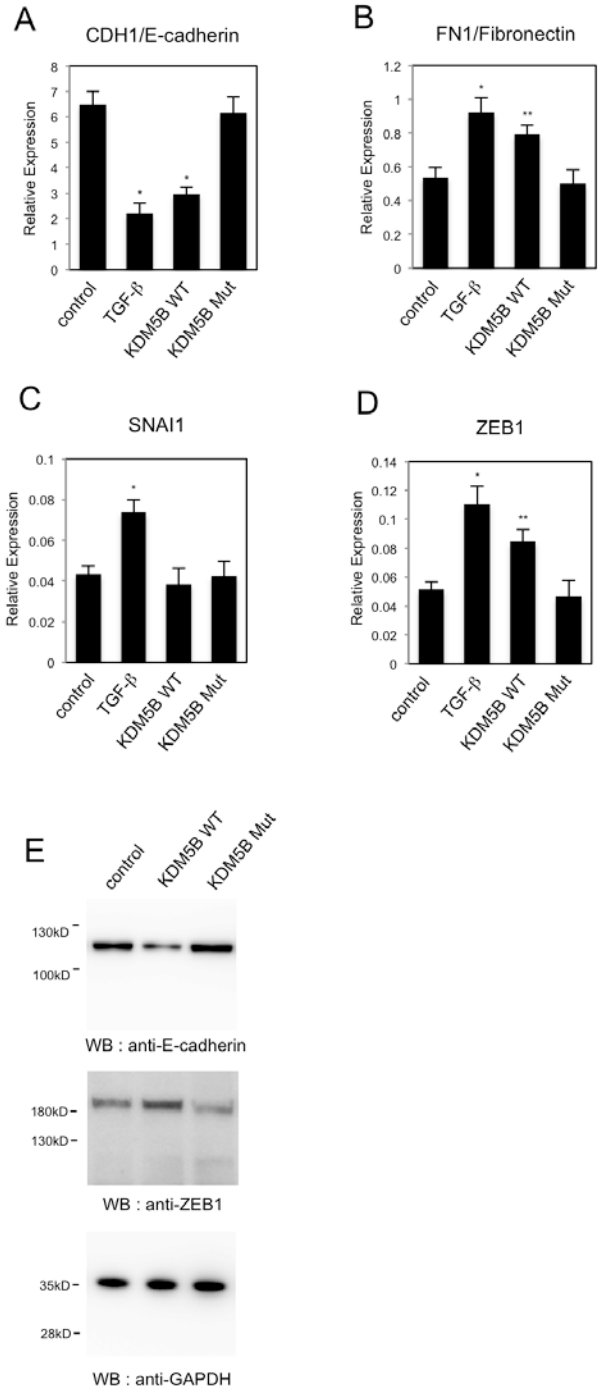

Enkhbaatar et al. Supplementary Figure 5

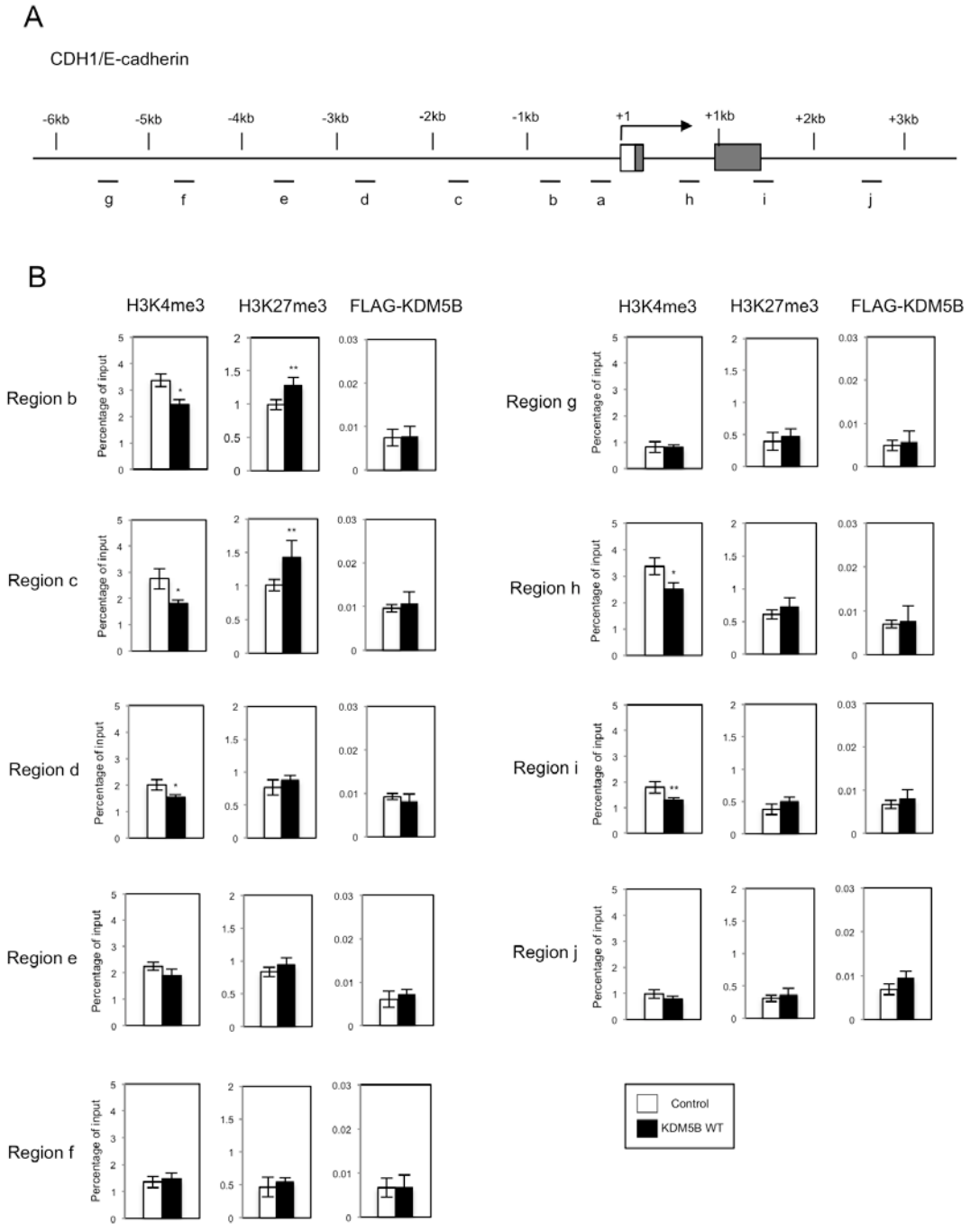

Enkhbaatar et al. Supplementary Figure 6

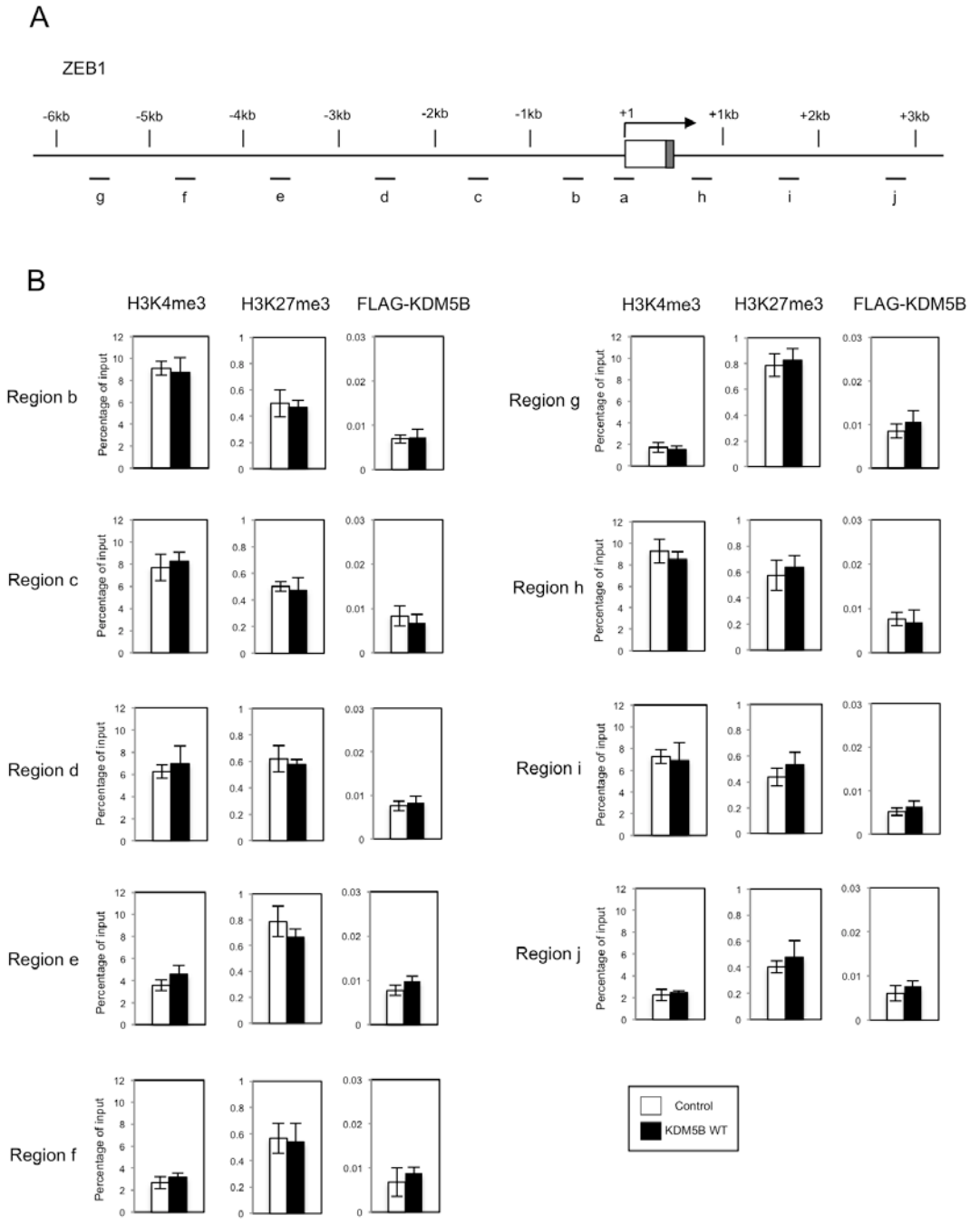

Enkhbaatar et al. Supplementary Figure 7

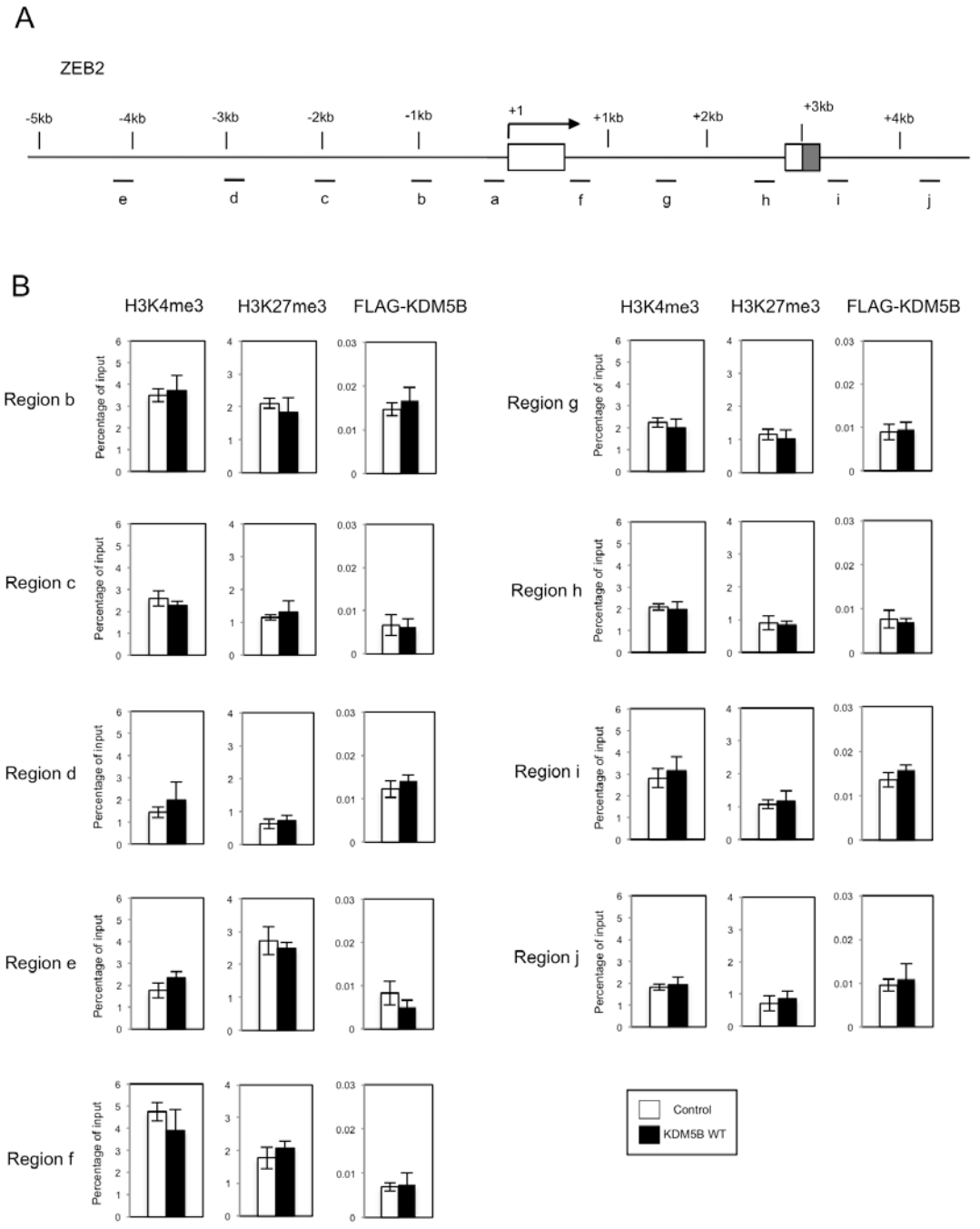

Enkhbaatar et al. Supplementary Figure 8

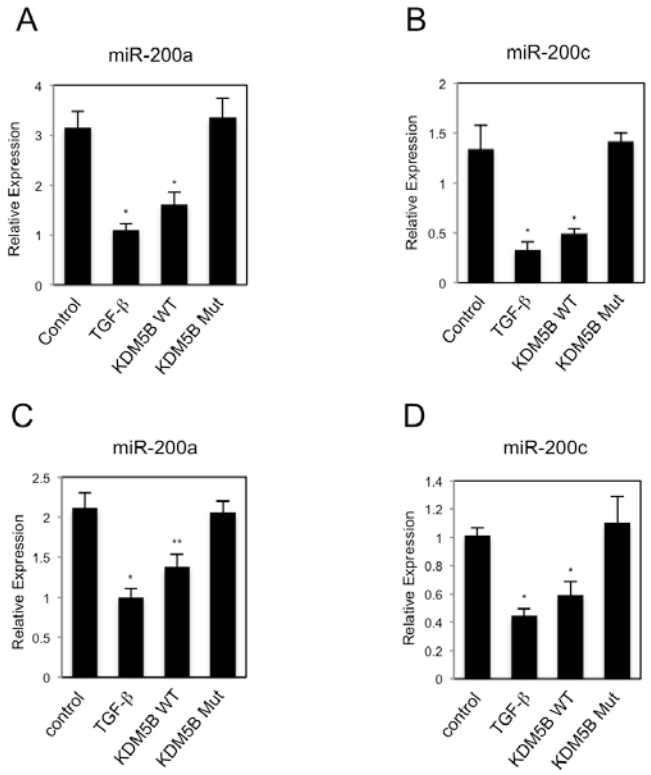

Enkhbaatar et al. Supplementary Figure 9

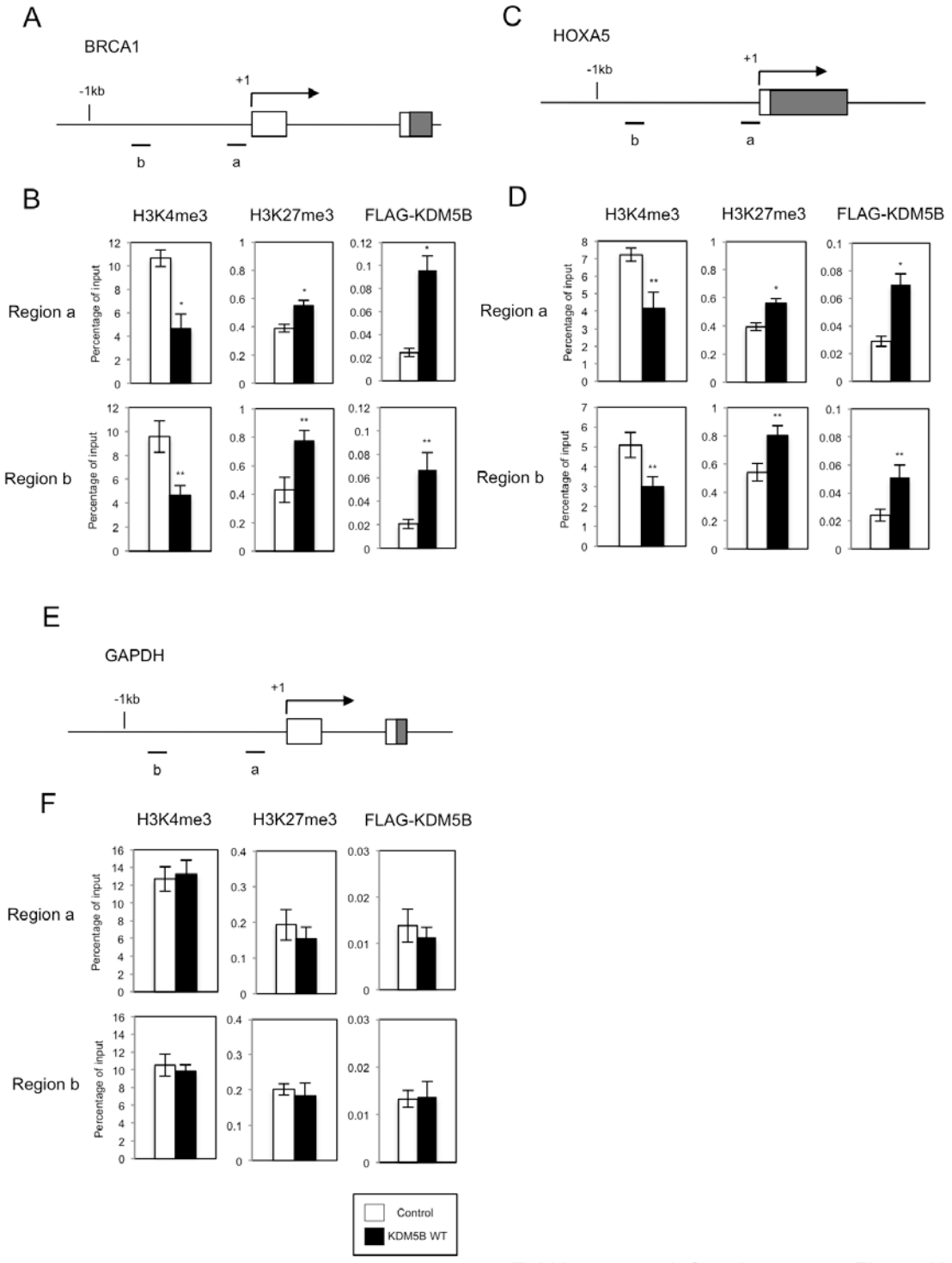

Enkhbaatar et al. Supplementary Figure 10

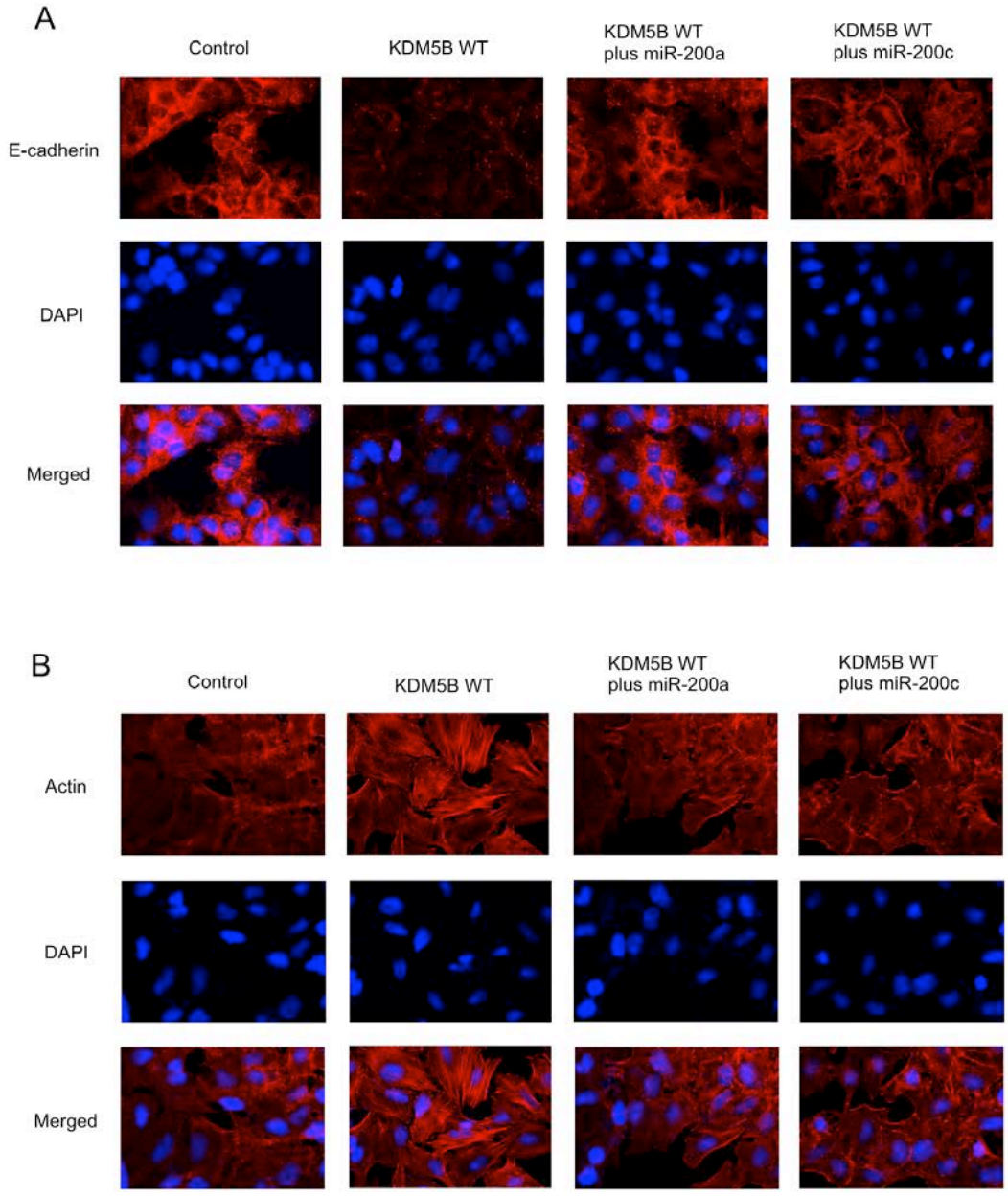

Enkhbaatar et al. Supplementary Figure 11

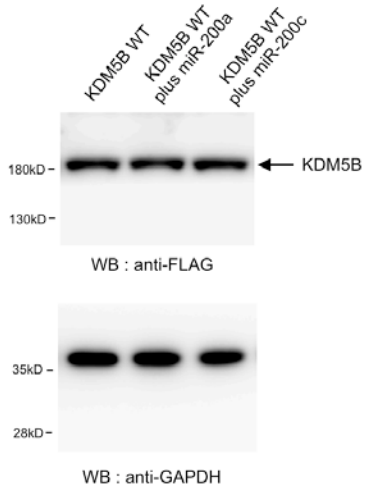

Enkhbaatar et al. Supplementary Figure 12

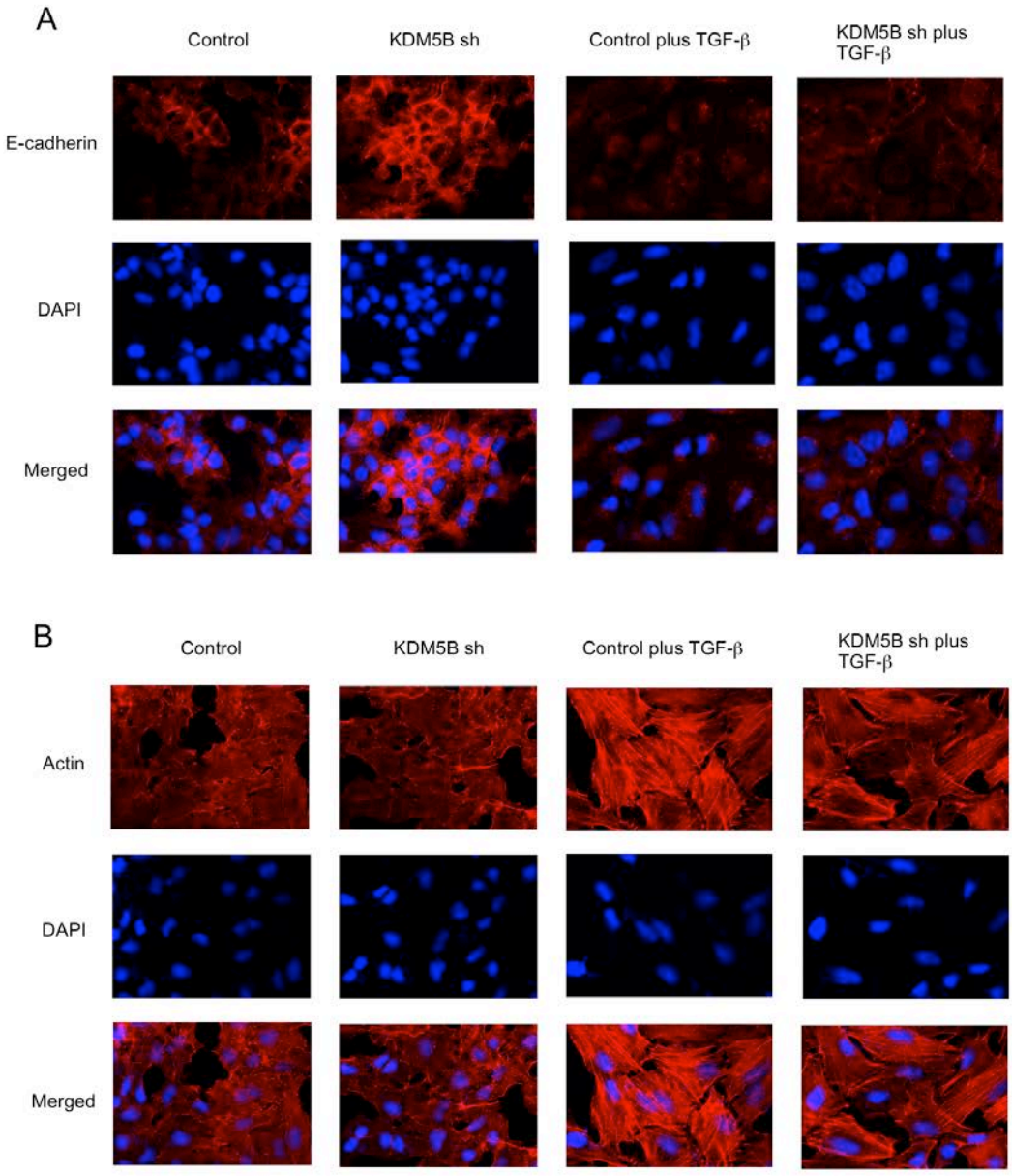

Enkhbaatar et al. Supplementary Figure 13

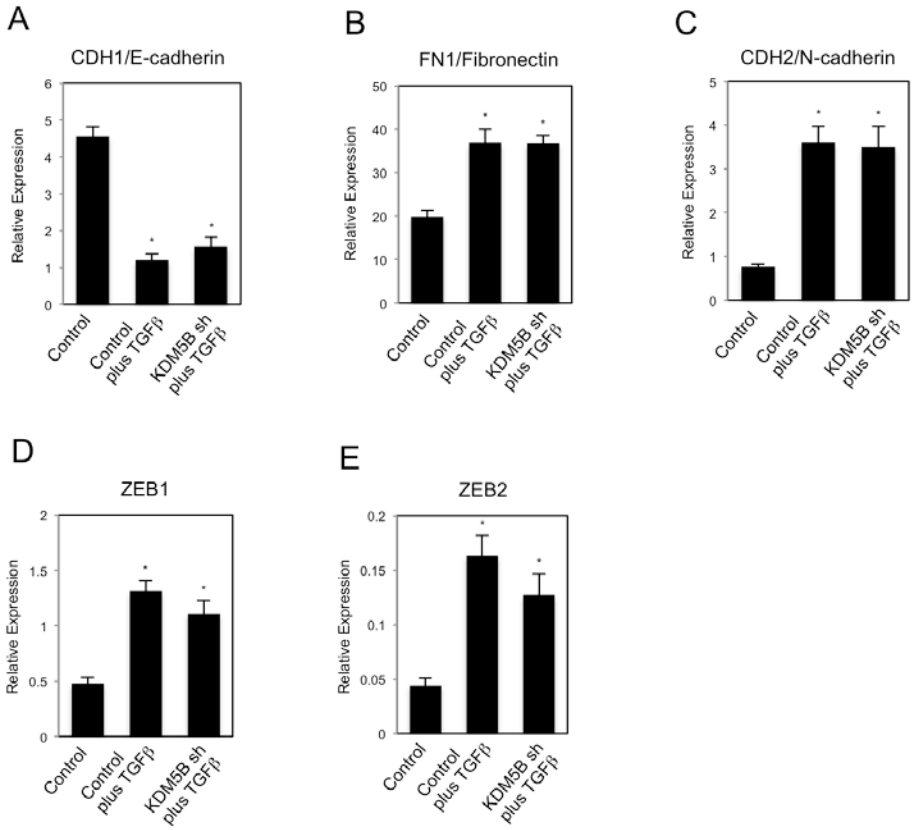

Enkhbaatar et al. Supplementary Figure 14

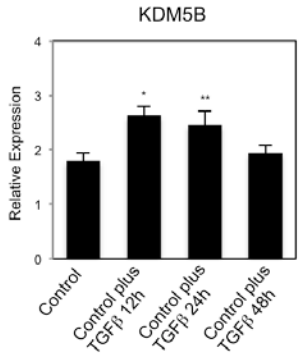

Enkhbaatar et al. Supplementary Figure 15